



Babeş-Bolyai University
Faculty of Chemistry and Chemical Engineering
Doctoral School of Chemistry



PhD Thesis Summary

Similarities of compounds with applications in energy storage systems

Ph.D. candidate: Dan-Marian JOIȚA

Scientific advisor: Prof. Lorentz JÄNTSCHI

CLUJ-NAPOCA
2024

Table of Contents

Abstract	1
Acknowledgements	3
Acronyms	4
List of publications	5
I. Introduction	8
II. General background	12
II.1. Energy storage systems	12
II.1.1. Historical facts that paved the way	12
II.1.2. Definitions and basic principles	13
Redox couples	13
Components	13
II.1.3. The first breakthroughs	15
II.1.4. Improvements are beginning to make sense	16
II.1.5. Types of energy storage systems	17
II.1.6. The determining steps	17
II.1.7. Emerging trends and prospects	19
II.2. Computational modeling	19
II.2.1. Computational methods	20
II.2.2. Structure-Property Relationships	20
II.2.3. Topological indices	22
II.3. Similarities of energy storage systems	23
II.3.1. Electron transfer mechanisms	25
II.3.2. Electrochemical properties	26
II.3.3. Performance metrics-parameters	26
III. Purpose, objective, and scope	27
Personal contributions	28
IV. Methods and results	29
IV.1. Polynomials in chemistry	29
IV.1.1. Characteristic polynomial	31
IV.1.2. Permanental polynomial	34
IV.1.3. Immanantal polynomial	35
IV.1.4. Discussion	36
IV.2. Extending the characteristic polynomial	37
IV.2.1. Materials and methods	38
Graphs, Matrices, and the Characteristic Polynomial	38
Characteristic Polynomial Extension	40
IV.2.2. Numerical case study	43
IV.2.3. Conclusions and further work	48
IV.3. Derivative-free families of with- and without-memory iterative methods for solving nonlinear equations and their engineering applications	49
IV.4. An application of the eigenproblem	51
IV.4.1. Materials and methods	52
IV.4.2. Geometrical similarities	55
IV.4.3. Discussion	57
IV.4.4. Improvements of the code	58

IV.4.5. Performance	58
IV.4.6. Further results of similarities	59
V. Final conclusions and outlook	117
Appendices	120
A File extension conversion procedure	120
B References management using Zotero	120
C Useful text editing examples	120
D BKChem examples	121
E Examples for using some databases	121
F Full version of Table IV.4.10	122
G Programming notes	141
H Final code	143
References	157

Table of Contents for Summary

I. Introduction	4
II. General background	6
II.1. Energy storage systems	6
II.2. Computational modeling	10
II.3. Similarities	14
PERSONAL CONTRIBUTIONS	17
IV. Materials and results	17
IV.1. Polynomials in chemistry	17
IV.2. Extending the characteristic polynomial	20
IV.4. An application of the eigenproblem	28
V. Final conclusions and outlook	38
References	40

Keywords: counting polynomials; extension; eigenproblem; eigenvalues; molecular alignment; orthogonal alignment; geometrical similarities; similarities; database; antisymmetric matrix; redox equilibria; energy storage systems.

I. Introduction

Understanding similarities between compounds involved in redox equilibria of energy storage systems could accelerate increase of performance. Researchers can discover materials that exhibit desirable properties, such as high energy density, fast charge/discharge rates, long cycle life, electrochemical efficiency, or integration.

Similarities could provide insights into the packing and arrangement of atoms within a compound. By identifying compounds with similar geometries to high-energy-density materials, researchers can explore alternative compounds that may exhibit similar or improved energy storage capabilities [1].

Compounds with similar geometries may exhibit similar:

- charge/discharge rates, allowing for faster energy storage and release due to the kinetics of redox reactions and electron transfer processes within energy storage systems;
- structural stability, resistance to degradation, and cycling performance;
- redox potentials and charge transfer characteristics, leading to improved electrochemical efficiency [2].

Computational modeling has brought some contributions to chemistry over the years, such as: efficiency and cost-effectiveness, material design and optimization, prediction of material properties, analysis and visualization. The latter is where we stop and try to bring a contribution. A few computational methods are mentioned, and topological indices are introduced. Another history lesson is now started for topological indices since polynomials are topological indices and molecular descriptors.

Similarities are exemplified followed by what it is hoped they can help discover.

The contribution of this thesis begins to be more practical in Chapter IV: Methods and results. Simple examples on how to calculate some polynomials for one compound of interest are presented. The characteristic polynomial of LiMn_2O_4 is calculated using the method of Sachs. The permanent and immanant polynomials are also presented.

Ways in which the characteristic polynomial can be extended are shown in the next section. A case study calculates area and volume for congeners of C_{20} fullerenes. Some of these possible examples could be used to replace parts of the algorithm of section IV.4.

The most experimental part of our effort is a Matlab script that can be used to search for geometrical similarities between compounds used in energy storage systems. The algorithm for finding similarities of compounds with applications in energy storage systems and its results are presented in subchapter IV.4. Some concepts are used such as:

- Databases are structured collections of data that are organized in a way that facilitates efficient data storage, retrieval, and management. They can establish relationships between different data entities, enabling the representation of complex data structures and associations.
- Structural alignment involves superimposing the three-dimensional structures of compounds to identify regions of structural similarity and to quantify the differences in their spatial arrangements.

- Quadratic matrix are square matrices (having an equal number of columns and rows) fundamental in the study of matrix operations, determinants, inverses, and eigenvalues.
- An antisymmetric matrix, also known as a skew-symmetric matrix, is a square matrix whose transpose is equal to its negative. All components are antisymmetric (their signs differ) relative to the main diagonal:

$$\begin{matrix} & 0 & a & b \\ -a & & 0 & c \\ -b & -c & & 0 \end{matrix}$$
 The eigenvalues of an antisymmetric matrix are purely imaginary or zero.
- Interpolation involves constructing a function that passes exactly through the given data points, allowing for the estimation of values at intermediate positions.
- Trilateration is a geometric technique employed to ascertain the position of a specific point by measuring its distance from three predetermined reference points.

We present how other programs achieve alignment. The eigenproblem is defined and these eigenvalues of the matrix are the roots of the characteristic polynomial. The extension of the characteristic polynomial to each Cartesian coordinate is utilized to rotate, translate and reflect until the candidate arrives in a position with the most elevated absolute eigenvalues for the Cartesian coordinates. Similar candidates are found by comparing sums of squared eigenvalues for the entire compound or combinations of fewer selected atoms. The eigenproblem algorithm aligns candidates. All previously striped atoms are attached using a trilateration script found in literature. An approximation is found for the characteristic polynomial of the matrix of the Cartesian distances on Ox. A sum is eventually calculated by using the law of motion of the rotation of a body about a fixed axis.

Improvements over the published algorithm of 2021 are presented. It may be noticed that the algorithm was initially used to align and superpose amino-acids. The possibility exists that the developed algorithm can be used to align anything in 3D space.

In the last chapter "Best" results of similarities between compounds with applications in energy storage systems are presented for 293 candidates. Parameters are introduced from databases and literature. Limitations and further improvements are discussed.

Time spent for each compound chosen for comparison can be 5 hours for 293 compared files and up to 15 atoms per file. This led to a total runtime of two years for the published algorithm in 2021. The writing of this thesis began when a timeframe of months was achieved through vectorisation of the code. The final version is 180 faster. Computer time increases by at least 6 hours for one file containing 16 atoms. In case similarities are found between compounds, more geometries can be downloaded and compared even though the files contain more than 15 atoms.

All these reductions still lead to many numbers. How could one choose the best similar results from all these numbers? The Matlab code is constructed to provide a hierarchy of all possibilities using a similar function to TM-score. The score is influenced by the number of atoms superposed.

For the first compound, 72 candidates were taken into account with scores > 0.85 . Some present exactly the same geometry and could be treated as coincidences. Parameters

are taken from “The Materials Project” database. From the second compound onwards, tables are merged and results of similarities are not presented visually. This is more practical in the aspect that tiny pictures for many compounds are hard to compare for the reader.

II. General background

II.1. Energy storage systems

This section provides an exploration of energy storage systems fundamentals, including the basic principles, components, and examples.

Redox couples

Reversible redox (reduction-oxidation) reactions involve the transfer of electrons between chemical species, enabling storage of electrical energy and conversion to chemical energy. They can be analogous to the case of conjugate acids and bases. For example in the Lewis theory, an acid is a substance that accepts electron pairs. When a reducing agent donates one or more electrons its oxidation number increases. In this case, we are speaking of single elements that undergo oxidation or reduction. The resulting species is capable of re-accepting the electrons and is now an oxidizing agent.

As in the case of acids and bases, a table of half-equations can be used to predict which way a redox reaction will proceed.

Energy density refers to the amount of energy that can be stored per unit mass or volume. The redox potential difference between two compounds in a redox couple determines the voltage of the energy storage system.

Multivalent metals offer more than one oxidation step that can potentially increase energy density. Polyprotic acids or bases are neutralized similarly in more dissociation stages. A well-known metal used with success in energy storage systems is vanadium. While charging a vanadium redox flow energy storage system, V(II) ions at the positive electrode are oxidized to V(III) ions, while V(V) ions at the negative electrode are reduced to V(IV) ions.

Components

Energy storage systems are composed of one or more electrochemical cells (voltaic piles), each containing an anode, a cathode, and an electrolyte. Chemical reactions generate a flow of electrons, creating an electric current that can be harnessed for various purposes.

The anode is the electrode where oxidation takes place during discharge (or use), and electrons are released into the external circuit, becoming positively charged ions or species. The cathode is the electrode where reduction occurs during use; accepting electrons from the external circuit and becoming negatively charged ions or species.

Electrolytes enable the movement of ions or species between the anode and cathode, allowing for the transfer of charge during operation. It ensures the continuity of the electrochemical reactions, the flow of electrons, charge and completes the electrical circuit.

The choice of anode material depends on the specific chemistry. Common anode materials include zinc, lithium, graphite, and lead. Common cathode materials include manganese dioxide, lithium cobalt oxide, nickel-cadmium compounds, and lead dioxide.

Electrolytes can be liquid (such as aqueous solutions or organic solvents), solid-state, or gel. Each type has its advantages and limitations, depending on the specific chemistry and application.

The chemical notation for a Zn/Cu cell is:

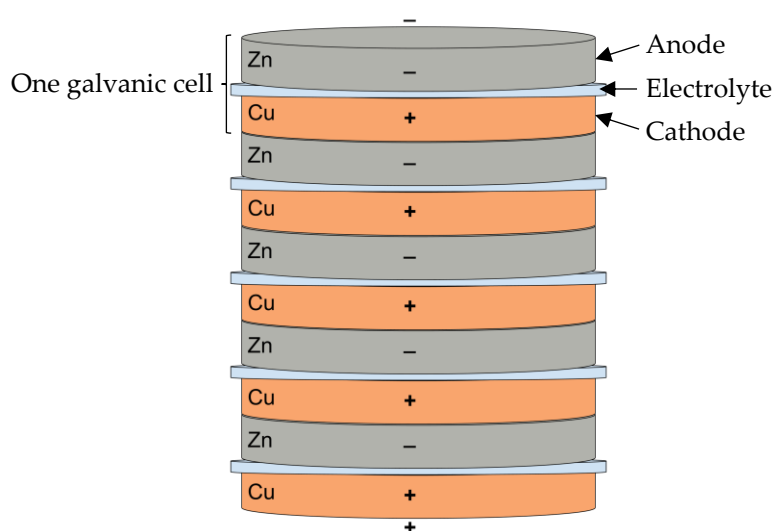


Figure II.1 Example of a series of Zn/Cu galvanic cells.

A half-cell is one of the two electrodes in an energy storage system (voltaic pile, galvanic cell or simple battery). For example, in the Zn/Cu battery, the two half-cells make an oxidizing-reducing couple. Placing a piece of reactant in an electrolyte solution makes a half-cell. Unless it is connected to another half-cell via an electric conductor and salt bridge, no reaction will take place in a half cell. During discharge, the positive electrode is a cathode, and the negative electrode is an anode.

Anode (-)



Zn is the reducing agent.

Zn is being oxidized to Zn^{2+} .

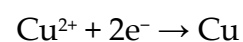


(+) Cathode



Cu^{2+} is the oxidizing agent.

Cu^{2+} is being reduced to Cu.



Now Zn^{2+} is the oxidizing agent (also known as an oxidant, oxidizer, electron recipient, or electron acceptor) and Cu is the reducing agent (also known as a reductant, reducer, or electron donor).

So, if we have a circuit connected through an electrolyte and an electric conductor, we can insert a light bulb to use the energy (as a potential difference U). After some time, equilibrium is achieved, the potential difference fluctuates close to zero and it is too small to keep the light bulb lit up.

The first Zn/Cu systems were non-rechargeable – primary systems. As time passed, it is now possible to create a secondary system that is rechargeable [42]. Roles change during recharge because oxidation takes place at the positive electrode, which we now call the anode, and reduction takes place at the negative electrode, which we now call the cathode.



Now Zn^{2+} is the reducing agent and Cu is the oxidizing agent.

And so on and so forth we use and recharge the battery.

Estimating the electrochemical cells potential is often given as example to students, and a course as such presents these principles in another way [43,44].

In the late 1780s, Luigi Galvani, an Italian physician and physicist, made a discovery known as "animal electricity". Through his experiments with frog legs, Galvani observed that the muscles of the frog legs would twitch when in contact with different metals. This discovery laid the foundation for understanding the relationship between electricity and living organisms [45].

Alessandro Giuseppe Antonio Anastasio Volta believed that a chemical interaction causes electricity since 1794. The true breakthrough in battery technology came in 1800 when he invented the voltaic pile. This early invention consisted of alternating layers of zinc and copper discs separated by cardboard soaked in saltwater. The voltaic pile was the first device capable of producing a continuous flow of electricity, marking a significant milestone in the field of electrochemistry. A pile of his belongings is displayed at the University History Museum of the University of Pavia [46].

In June 1814 Volta met Michael Faraday in Milan and gave him one battery.

Faraday made significant contributions to the understanding of electrochemistry in the 1830s. He formulated the laws of electrolysis, which describe the relationship between the amount of chemical reaction occurring at an electrode and the amount of electricity passing through the electrolyte. He conducted experiments with a ferrite ring, a galvanometer, and a battery; and also developed the principle of ionic mobility in chemical reactions of batteries. Faraday's laws provided a fundamental understanding of the electrochemical processes that occur.

A Clarendon Dry Pile of uncertain composition is kept at Oxford University. It is called The Oxford Electric Bell. It has certainly been ringing since 1840, and may have been ringing since 1825. It will stop in approximately one decade [47].

More chemistries have emerged. We have constructed a Table.II.1 to name a few:

Primary systems refer to non-rechargeable inventions that are designed for single-use. Once the chemical reactions are exhausted, it is no longer usable and must be replaced. They utilize various chemistries, including alkaline, zinc-carbon, and lithium. They are self-contained power sources and are commonly used in devices with low power requirements, such as remote controls and disposable electronics. They generally have higher energy density than secondary ones, but fuel cells can offer even higher energy density depending on the fuel used.

Secondary storage systems have the rechargeability advantage, employing various chemistries, including lead-acid, lithium-ion, nickel-metal hydride (NiMH), and nickel-cadmium (Ni-Cd). They are our main subject [61].

Fuel cells continuously generate electricity through the electrochemical reaction between a fuel (such as hydrogen) and an oxidant (such as oxygen). There are several types of fuel cells, including hydrogen fuel cells, direct methanol fuel cells (DMFC), and solid oxide fuel cells (SOFC). Each type utilizes different fuels and operates at different temperatures. They have diverse applications, including transportation (fuel cell vehicles), stationary power generation, portable power sources, and even space exploration. They offer high energy efficiency, low emissions, and the potential for using renewable fuels [62].

Multifunctionality: Paint-On, Flexible, Stretchable, and Self-Charging Batteries are some examples of a system that tries to occupy a space that we do not use in our lives. Researchers are exploring technologies that can also perform sensing, actuation, or self-healing functions [75].

Supercapacitors: Also known as ultracapacitors, they store energy through the electrostatic adsorption of ions at the electrode-electrolyte interface. The geometric arrangement of electrode materials plays a crucial role in determining the specific surface area available for ion adsorption. Materials with a high surface area, such as activated carbon or graphene, provide more sites for ion adsorption, resulting in higher capacitance and energy storage capacity [76].

Recently, aqueous organic RFBs (AORFBs) and non-aqueous organic RFBs (NAORFBs) have received increasing attention as viable alternatives [77].

Recycling and Sustainability: As the demand for storage systems continues to grow, there is a focus on developing sustainable and environmentally friendly technologies. This includes efforts to improve the recycling processes, reduce the use of scarce and toxic materials, and promote circular economy practices in the industry. Although the environment is very important for us, some implications will only be mentioned since the subject does not adhere to the scope of this thesis: Raw Materials, Energy Consumption, Lifespan, End-of-

Life Management, Toxic Materials, Hazardous Waste, Policy and Regulations. Computational chemistry avoids resource waste since experiments with no benefit are avoided, although it is physically impossible to try all combinations of materials in any given acceptable time [78].

II.2. Computational modeling

Efficiency and cost-effectiveness: Traditional experimental methods for discovering and optimizing materials can be time-consuming, expensive, and resource-intensive. Computational methods offer a more efficient and cost-effective approach by allowing researchers to screen and analyse a number of potential materials before conducting physical experiments. Some effort was putted in various computational modeling techniques [79–84].

Material design and optimization: Computational methods enable researchers to design and optimize materials with specific properties and performance characteristics. Through simulations and modeling, researchers can predict the behaviour of materials at the atomic and molecular level, understand their electrochemical properties, and identify promising candidates for further investigation.

Understanding electrochemical processes: Computational methods provide insights into the underlying electrochemical processes that occur. They can simulate and analyse the movement of ions, electrons, and defects within the materials, helping researchers understand the mechanisms that govern performance and degradation. This knowledge is crucial for developing strategies to enhance performance and durability.

Prediction of material properties: Computational methods can predict various material properties relevant to performance, such as voltage, capacity, stability, and diffusion coefficients. These predictions guide experimental efforts by narrowing down the search space and focusing on materials with the highest likelihood of success.

Accelerating material development: By combining computational methods with experimental techniques, researchers can accelerate development of new materials. Computational predictions can guide the synthesis and characterization of materials, reducing the trial-and-error approach and enabling more targeted and efficient material design.

Visualization and analysis: Computational modeling enables the visualization and analysis of complex geometrical structures in energy storage systems. Advanced visualization techniques, such as three-dimensional rendering and virtual reality, allow researchers to explore and understand the intricate details of materials' geometric arrangements. This visual understanding aids in identifying patterns, correlations, and relationships between geometrical similarities and electrochemical properties.

Molecular dynamics (MD) simulations can be employed to investigate the geometric arrangement of atoms and molecules within energy storage materials. By simulating the behaviour of atoms and molecules over time, MD simulations can provide insights into the structural stability, diffusion pathways, and interfacial properties of materials. This infor-

mation helps researchers understand how similarities impact the performance and behaviour of energy storage systems.

DFT calculations are widely used to study the electronic structure and properties of materials. By applying DFT, researchers can analyse the geometric arrangement of atoms and calculate various properties, such as band structures, charge densities, and redox potentials. This information aids in understanding how similarities influence the electronic properties and charge transfer mechanisms within energy storage materials.

Computational modeling techniques, such as molecular optimization algorithms and Monte Carlo simulations, can be used to optimize the geometric arrangement of materials. By iteratively adjusting the positions and orientations of atoms or molecules, researchers can find the most favourable configurations that maximize specific properties, such as surface area, porosity, or interfacial interactions. This optimization process helps in tailoring the geometrical characteristics of materials to enhance their electrochemical performance.

Structure-property relationships (SPR) refer to the connections between the structural characteristics of a material or system and its resulting properties or behaviour. In the context of energy storage systems, understanding these relationships is crucial for designing and optimizing materials and devices with desired performance. Here are some examples of structure-property relationships in energy storage systems:

The crystal structure of electrode materials or catalysts in fuel cells can significantly impact their electrochemical performance. For example, in lithium-ion chemistry, the crystal structure of the cathode material, such as LiCoO_2 , affects its specific capacity, cycling stability, and rate capability. Similarly, in fuel cells, the crystal structure of catalysts, such as platinum nanoparticles, influences their catalytic activity and efficiency in oxygen reduction or hydrogen oxidation reactions [85].

The morphology and surface area of materials play a crucial role in energy storage systems. For instance, in supercapacitors, materials with a high surface area, such as activated carbon or graphene, provide more active sites for charge storage, leading to higher capacitance. Similarly, in lithium-ion designs, nanostructured electrode materials with a large surface area can enhance the diffusion of lithium ions, improving performance [86].

The porosity of materials in energy storage systems affects the transport of ions or molecules within the system. Porous materials with well-defined pore structures can facilitate the diffusion of ions, enhancing the charge and discharge rates. In fuel cells, the porosity of the electrode materials can impact the accessibility of reactants to the catalyst surface, influencing the overall reaction kinetics [87].

The structure and properties of interfaces between different materials or phases within an energy storage system can impact its stability and performance. In lithium-ion chemistry, the solid-electrolyte interphase (SEI) formed at the electrode-electrolyte interface plays a crucial role in stability and cyclability. The structure and composition of the SEI layer can affect ion transport, charge transfer, and overall performance [88].

Vacancies and impurities in crystal structures of materials can influence their charge transport properties. In energy storage systems, defects can affect the diffusion of ions or electrons, leading to changes in conductivity, capacity, or reaction kinetics.

Polynomials are related to SPR by the application of combinatorial mathematics to enumerate and characterize the diverse molecular configurations and their associated properties. Polynomials provide a systematic framework for analysing the structural motifs, similarities, and their impact on the resulting properties of chemical systems. By leveraging polynomials, researchers can gain insights into the relationships between molecular structures and their properties, thereby contributing to the understanding of structure-property relationships in chemistry.

In the context of redox equilibria, for example, polynomials can be applied to analyse the geometric arrangements of compounds, the distribution of electron transfer pathways, and the resulting electrochemical properties. This approach allows for the systematic enumeration and characterization of molecular configurations, providing a quantitative basis for understanding the relationships between structural motifs and redox behaviour. By integrating polynomials into the exploration of structure-property relationships, researchers can gain a deeper understanding of how the geometric arrangements of molecules influence their electronic properties, reactivity, and overall behaviour in redox processes.

Overall, the application of polynomials in chemistry offers a unique perspective on structure-property relationships by providing a quantitative and systematic approach to analyse the interplay between molecular structures and their resulting properties. This approach holds promise for unravelling the intricate connections between geometry, electronic structure, and material properties, ultimately contributing to the advancement of materials design, catalysis, and the rational design of functional molecular systems.

As Diudea well said, a single number, representing a chemical structure in graph-theoretical terms, is called a topological index (TI) [89]. A topological index is a real number related to a molecular graph [90]. Many nanomaterials, drugs, and crystalline materials appear in various industries. Medical behaviour can be studied with TIs, leading to quantitative structure property relationships (QSPR) and quantitative structure activity relationships (QSAR) [91,92]. The first TIs, even before the introduction of the term, are those of Calingaert and Hladky in 1936 [93], Kurtz and Lipkin in 1941 [94], and of Wiener in 1947 [95]. Degree-based TIs are the most studied [96].

Some of the first names to speak about chemical graphs are enumerated by Rouvray [97]: Newton, Macquer, Boscovich, Lomonosov, Cullen, and Higgins. In 1808, Dalton and Wollaston introduced the ball and stick models used in classrooms [98,99]. One of the first chemists to try a prediction of properties was Koop in 1844 [100]. Leading the way into the valence concept, Couper drew the first bond between atoms in 1858, and Frankland had the first idea about valences in 1864. Kekulé's first attempt to depict the tetrahedral carbon followed in 1867 [97]. Cayley, in 1874 [101,102], and Sylvester, in 1875 [103], drew the first

chemical graphs. Werner studied complex chemistry in 1893 [97]. During the 1930s many new molecules were synthesized. Chemical graphs became more of a must in order to differentiate this relatively large number of new molecules. In 1937, Polya incorporated the concepts of symmetry classes, permutation groups, and generating functions in his Enumeration Theorem [104] by continuing an earlier work of Cayley [102].

Returning to TIs, two more initial indexes were studied: F by Platt in 1947 [105,106] and N_2 by Scantlebury in 1964 [107], before Hosoya showed that W is the half sum of all entries in $[Di]$ and afterwards proposed the Z index in 1971 [108], which he first attributed to Wiener. The Zagreb index (M_1) followed in 1975 [109], which can be related to the Platt and Gordon–Scantlebury by: $F=2N_2=M_1-e$. Balaban followed with his Centric index in 1979 [110]. Danail Bonchev, Ovanes Mekenyan, and Milan Randić proposed a generalization of the graph centre concept to cyclic graphs in 1980 [111–113]. A way of classifying TIs is the grade of degeneration, and so we mention another of the first generation, proposed by Schultz in 1989 [114,115]. The beginning of the second generation is marked by the molecular connectivity index of Randić in 1975 [116], which was characterized by a very low degeneracy. To name another few: the high-order molecular connectivity indices studied by Kier and Hall in 1975 [117–120]; the information–theoretic indices of Bonchev and Trinajstić in 1977 [121]; the Merrifield and Simmons indices that were studied in 1980 [122–124]; in an effort to decrease degeneracy, Mekenyan and Trinajstić proposed the topological information super-index in 1981 [125]; in 1982, Balaban modified the Randić formula and gave rise to the average distance-based connectivity index [126]; the information–theoretic indices of Basak and co-workers in 1983 [127]; orbital information index for graph connections of Bertz in 1988 [128]; or the electro-topological state indices of Kier and Hall in 1990 [129,130]. A contribution to the idea of using Eigenvalues as TIs was coined by Lovasz and Pelikan in 1973 [131].

The third generation of TIs may be considered to start by defining real-number local vertex invariants (LOVIs) [132], as detailed by Devillers and Balaban in a book chapter [133]. Gutman has summarized the main properties of molecular-graph-based structure descriptors and provided a critical comparative study [134]. Since then, a few indices have been developed: a type of Zagreb index based on degrees of neighbours of vertices [135]; an eccentric atom–bond connectivity index [136]; a Sanskruti index $S(G)$, showing good correlation with entropy of an octane isomer [137]; the multiplicative atom–bond connectivity index [138]; the product connectivity leap index [139]; M_N as a neighbourhood Zagreb index of product graphs [140]; and so on. Many authors have computed indexes for different applications [141–143], or analytical expressions for such indexes [144–148]. A number of TIs are based on polynomial coefficients and can be derived directly or by using integrals or derivatives [142,149].

II.3. Similarities

One example of similarity is observed in transition metal oxides used as electrode materials in lithium-ion batteries. These materials often adopt a layered crystal structure, with transition metal ions arranged in a specific pattern. The geometric arrangement of these ions influences the diffusion pathways for lithium ions during charge and discharge cycles, affecting the capacity, cycling stability, and rate capability [150].

Another example is found in redox-active organic molecules used in flow systems. These molecules often possess a specific molecular framework, such as quinones or viologens, which allows for reversible redox reactions. The geometric arrangement of functional groups within these molecules can influence their solubility, stability, and redox potentials, ultimately impacting the efficiency and performance of the flow system [151].

In lithium-ion chemistry, the geometric arrangement of electrode materials can impact the diffusion pathways for lithium ions during charge and discharge cycles. Materials with a layered crystal structure, such as LiCoO_2 or $\text{LiNi}_x\text{Mn}_y\text{Co}_{1-x-y}\text{O}_2$ (Li-NMC), provide pathways for efficient lithium ion transport, enhancing performance [152].

Lithium-sulphur chemistry is a promising alternative to traditional lithium-ion due to its high theoretical energy density. The geometric arrangement of sulphur and lithium in the cathode and anode materials can influence sulphur utilization, lithium diffusion, and overall performance [153].

Sodium-ion chemistry also exhibits geometrical similarities in possible electrode materials. Compounds such as NaMnO_2 or $\text{NaNi}_{0.5}\text{Mn}_{0.5}\text{O}_2$ adopt layered structures, allowing for reversible intercalation of sodium ions during charge and discharge cycles [154].

Solid-State chemistry: The geometric arrangement of the solid electrolyte material can impact its ionic conductivity. Materials with a crystalline structure, such as lithium garnet ($\text{Li}_7\text{La}_3\text{Zr}_2\text{O}_{12}$) or sulphide-based electrolytes, provide pathways for efficient ion transport, improving performance and safety [155].

Vanadium redox flow chemistry: VRFBs use vanadium ions in different oxidation states to store and release energy. The geometric arrangement of vanadium ions in electrolyte solution can impact efficiency, capacity, and reduced energy losses - by optimizing geometrical configuration of the electrolyte flow channels [156].

Organic redox flow chemistry utilizes redox-active organic molecules as active species in the electrolyte. Geometric arrangement of functional groups within these molecules can influence their solubility, stability, and redox potentials, ultimately impacting efficiency and performance of the flow system.

Sodium-ion capacitors combine the high power density of supercapacitors with the energy density of sodium-ion design. The geometric arrangement of the sodium-ion intercalation materials, such as hard carbon or transition metal oxides, can impact the capacity, rate capability, and cycling stability of the sodium-ion capacitor [157].

Metal-halide chemistry: sodium-iodide, zinc-bromine or zinc-chlorine designs utilize metal ions and halide ions in the electrolyte to store and release energy. The geometric arrangement of the metal and halide ions can affect the solubility, redox reactions, and overall performance. The crystal structures of the metal-halide compounds influence their solubility, redox reactions, and overall performance [158].

Lithium-oxygen / Li-O₂ / lithium-air chemistry has the potential for high energy density. The geometric arrangement of oxygen and lithium electrodes can impact oxygen diffusion, reaction kinetics, and overall efficiency [159].

Graphite anodes in lithium-ion chemistry: Graphite is commonly used as the anode material in lithium-ion designs. Its layered structure allows for the intercalation of lithium ions during charging and discharging cycles. Structurally similar graphite materials, such as natural graphite, synthetic graphite, or graphene, may possess similar specific capacity, rate capability, or cycling stability [160].

Perovskite cathodes in solid oxide fuel cells: Perovskite structures have a general formula of ABO₃, where A and B are metal cations. Structurally similar perovskite materials, such as lanthanum strontium manganite (LSM), lanthanum strontium cobaltite (LSC), or lanthanum strontium ferrite (LSF), may possess similar oxygen reduction reaction kinetics, ionic conductivity, or overall cell performance [161].

Metal-organic frameworks (MOFs) are porous materials composed of metal ions or clusters coordinated with organic ligands. MOFs have a highly ordered structure with a large surface area, making them suitable for applications in gas storage, catalysis, and energy storage. Structurally similar MOFs may possess similar porosity, surface area, or gas adsorption capacities [162].

Nanoscale structures in supercapacitors: Supercapacitors often utilize nanoscale structures, such as carbon nanotubes or graphene, as electrode materials. Structurally similar such nanomaterials may possess similar surface area, electrical conductivity, or ion diffusion kinetics, which directly impact the capacitance and energy storage capabilities of the supercapacitor [163].

The geometric arrangement of electrode materials in batteries can influence the electron transfer mechanisms during charge and discharge cycles. For example, in lithium-ion chemistries, materials with a layered crystal structure, such as lithium cobalt oxide (LiCoO₂) or lithium nickel manganese cobalt oxide (NMC), provide pathways for efficient electron and ion transport. Geometric arrangement of these materials allows for easy intercalation and de-intercalation of lithium ions, facilitating electron transfer between electrodes [164].

Geometric configuration of catalysts in fuel cells can impact the electron transfer mechanisms during the oxygen reduction reaction (ORR) and oxygen evolution reaction (OER). Catalysts with a high surface area and a well-defined geometric structure, such as platinum nanoparticles supported on carbon, provide more active sites for the ORR and

OER. The geometric arrangement of these catalysts can enhance the electron transfer kinetics and improve the overall efficiency of the fuel cell [165].

In supercapacitors, the geometrical structure of the electrolyte can affect the electron transfer mechanisms at the electrode-electrolyte interface. For example, the use of nano-porous carbon electrodes with a high surface area and a well-defined pore structure allows for a larger contact area between the electrode and the electrolyte. This facilitates the adsorption and desorption of ions, enabling efficient electron transfer and enhancing the capacitance of the supercapacitor [166].

Geometric arrangements of redox-active molecules in the electrolyte can impact the electron transfer mechanisms during charge and discharge cycles. The arrangement of functional groups within these molecules can influence their redox potentials and electron transfer kinetics. By optimizing the geometric configuration of the redox-active molecules, researchers can enhance the electron transfer efficiency and improve overall performance of the flow system [167].

The geometric surface area of electrodes in energy storage systems, such as batteries and supercapacitors, directly influences their capacitance. Increasing the surface area by utilizing nanostructured or porous materials enhances the electrochemical active sites available for charge storage and improves the overall capacitance of the system [168].

Geometric arrangements of materials in energy storage systems affect the diffusion pathways for ions, such as lithium or sodium ions, within the electrodes and electrolytes. Well-defined pathways with optimized geometries facilitate faster ion transport, leading to improved charge and discharge rates and overall electrochemical performance [169].

Geometrical similarities in the arrangement of redox-active species, such as transition metal ions or organic molecules can impact the kinetics of redox reactions in energy storage systems. The geometric configuration of these species influences their accessibility, proximity, and interaction with the electrolyte, affecting the reaction rates and overall electrochemical performance [170].

The geometric arrangement of materials can also influence the stability and cyclability of energy storage systems. In lithium-ion chemistry, the geometric structure of electrode materials can affect the stability of the solid-electrolyte interphase (SEI) layer, which forms on the electrode surface and impacts long-term performance and cycle life [171].

At the electrode-electrolyte interface, the geometric arrangement of materials can impact the charge transfer resistance in energy storage systems. A well-designed geometric interface with optimized contact and interfacial area reduces the resistance to charge transfer, improving the overall efficiency and performance of the system [85].

Energy density is a measure of the amount of energy a system can store per unit volume or weight.

Power density refers to the rate at which a system can deliver electrical power and is crucial for applications that require high power output.

The potential difference between the anode and cathode, determined by the redox reactions, is expressed in voltage. Capacity refers to the amount of electrical energy the system can store and is typically measured in ampere-hours (Ah) or milliampere-hours (mAh). The electrolyte's ability to facilitate ion transport contributes to energy storage capacity.

Researchers explore new materials for anodes and cathodes to enhance energy density, cycle life, and safety. Solid-state electrolytes and other advanced electrolyte materials are being developed to improve performance, stability, and safety. Optimizing the interfaces between the anode, cathode, and electrolyte is crucial for enhancing efficiency and longevity.

PERSONAL CONTRIBUTIONS

IV. Materials and results

The results of the last chapter will be making use of the following concepts discussed in this chapter. In recent years, the fields of chemistry, mathematics, and engineering have seen significant advancements in the development of methods and algorithms for solving complex problems. We will be exploring molecular descriptors, or algorithms for comparing and aligning molecular structures. These articles delve into the intricacies of their respective subjects, offering insights into research and developments in these fields. We highlight the significance of graph-theoretical polynomials in theoretical chemistry and their intersection with pure mathematics, showcasing the interdisciplinary nature of this research. We discuss various techniques, such as rotation-invariant techniques, fragment-based approaches, and dynamic programming algorithms, aimed at identifying regions of similarity and achieving fast and accurate structural alignments of molecules.

IV.1. *Polynomials in chemistry*¹

Haruo Hosoya first introduced a counting polynomial, the Hosoya polynomial (HP), to characterize a graph [108,173]. Counting matrices are the expanded forms of counting polynomials [174], since some distance-related properties can be expressed in the polynomial form with coefficients calculated from matrices [175,176].

Count-polys are very useful for discriminating among similar structures [177]. However, a polynomial is a more general treatment than an index. The advantage of polynomials is the reduction of degeneration since it is an invariant relative to the numbering of the atoms [177,178]. Degeneration refers to equal values for different molecules: the molecular weight has high degeneracy since there are many molecules with the same weight; 3D descriptors show low or no degeneracy at all since two molecules with the same weight can have their atoms arranged differently in 3D space. Formulas were obtained for entropies and energies of counting polynomials of some repeated structures f[179].

¹ Joița, D.-M.; Tomescu, M.A.; Jäntschi [172].

Given this, count-polys are molecular descriptors. They should be invariant to all the operations related to molecule manipulation that do not affect the molecular structure. Their number has increased in order to keep pace with large databases, such as CAS, so a few qualities should be sought when choosing descriptors. They should be: invariant to atom labelling and numbering; invariant to the molecule roto-translation; have an unambiguous algorithm; direct structural interpretation; and be locally defined [149,181]. Even more, they preferably are: theoretical and not based on experimental properties; not trivially related to other descriptors; generalizable to “higher” descriptors; efficient to construct; applicable to a broad class of molecules; interpretative by structure; use familiar structural concepts; change gradually with gradual change in structures; have the correct size dependence, if related to the molecule size; have good correlation with at least one property; and preferably discriminate among isomers.

Coefficients of polynomials and their zeros are of interest in chemistry [180]. Zeros are denoted by “ λ ” or “ x ” and are the same as roots (characteristic values, characteristic roots, latent roots, eigenvalues, proper values, or spectral values) [182]. Since many of the polynomials discussed are derived from matrices, defining the companion matrix is already solved. In other words: say we have an initial polynomial P_i , we require a matrix whose characteristic polynomial (the *ChP* discussed in this text) is the same as P_i ; based on the definition, the roots of this polynomial are identical to the eigenvalues. If one tries to describe the topology of a molecule, one can store information about the adjacencies (the bonds) between atoms as well as the identities (the atoms). Simplifying by disregarding the bond and atom types, the adjacency matrix ($[Ad]$ a matrix of elements $b_{i,j}=1$ if an edge connects vertices i and j and $b_{i,j}=0$ otherwise) and the identity matrix ($[Id]$) contain only zeros and ones. Any such or derived square matrix ($[Tm]$) can be used to construct a counting polynomial that carries features of the originating molecule:

$$CoP \stackrel{\text{def}}{=} \sum_{k \geq 0} n \cdot x^k, \quad (1)$$

where “ k ” is any value in $[Tm]$, “ n ” counts the occurrences of “ k ”, $n = \text{count}([Tm]_{i,j} = k)$, and “ x ” represents the roots of the polynomial [177,183]. For example, let there be:

$$[Tm] = [Id] = \begin{pmatrix} 1 & 0 \\ 0 & 1 \end{pmatrix}$$

Since both “1” and “0” occur two times:

$$CoP_{[Id]} = 2x^1 + 2x^0$$

Applications for calculating polynomials can rely on files containing molecular data, such as some gateways of software [184]. These are harder to maintain since there are many file extensions and programs that do not export identical files for the same chemical compound. Also, users should send their contributions if they fix any bugs so that the initial author can implement these improvements. Searching the Internet can reveal ways to calculate polynomials, but scripts need to be able to account for symbolic mathematics [185–187].

Rouvray [188,189] attracted attention to the scientific community in 1971 that interdisciplinary studies are indispensable to advance QSAR and QSPR. Today, we can look back at the day where we noticed that experimental studies are too slow to rely on for the discovery of compounds. Now computers are too slow and need to somehow use the advantages of the human mind to take a bigger step into predicting. Recent effort has been initiated to overcome this issue, but we do not know if the approaches are fruitful [190,191]. Machine learning takes some steps into this realm since we program computers to learn patterns we believe will lead to important scientific discoveries [192–194]. It is true that young minds prefer to see fast and easy results before understanding the core of complicated mathematics behind programs.

Being the most popular and most extensively studied polynomial in chemical graph theory, it is also found in literature by the terms, secular function or determinantal polynomial, and commonly denoted by ϕ or *ChP*. It is not a counting polynomial.

The first use of the *ChP* in relation with a chemical structure appeared after the discovery of wave-based treatment at the microscopic level. The *ChP* finds its uses in the topological theory of aromaticity, structure–resonance theory, quantum chemistry, counts of random walks, as well as in eigenvector–eigenvalue problems [197].

Its classic definition is simple:

$$ChP = \det(x \cdot [Id] - [Ad]) = |x \cdot [Id] - [Ad]| \quad (2)$$

Although not a counting polynomial, an elegant counting method of finding the *ChP*, in a limited number of cases, is that of Sachs [198]. A Sachs graph can be composed of isolated edges, rings, or combinations. We denote them with B_2 (“2” being the number of vertices an isolated edge can have) and R_m (“m” being the number of vertices a ring is composed of). The number of isolated edges = o and the number of rings = p . There is one restriction in the definition of a Sachs graph: $2 \cdot o + p \cdot m = k$, where k = the number of vertices. Let S_k be the set of all Sachs subgraphs (s) with “ k ” vertices of any graph G , and “ a ” being the total number of vertices of G . The number of components of the Sachs subgraph is $c(s)$ and the number of rings $r(s)$. The definition of *ChP* is:

$$ChP_G = \sum_{k \geq 0} \sum_{s \in S_k(G)} (-1)^{c(s)} \cdot 2^{r(s)} \cdot x^{a-k} \quad (3)$$

Liu and Zang found that the *ChP* characterizes paths and even cycles. Those cannot be characterized by the permanental polynomial [199].

The roots of the *ChP* are obtained by diagonalizing the adjacency matrix [180]. The sum of the w^{th} powers of these roots is equal to the w^{th} spectral moment of a graph. The coefficients of the *ChP* can be deduced from the spectral moments, and vice versa [149].

Ghosh developed formulas to calculate the coefficients of the *ChP* quickly and efficiently for the molecules represented by three classes of graphs. Later, they used the *ChP* and graph squaring to derive analytical eigen-spectra for graphs of linear chains and cycles

with alternant edge weights. These methods can be applied to all graphs having unit cells that are repeated along the molecule [200,201].

Mondal and Mandal have made some progress in obtaining the concentration vectors of reaction networks by finding an analytical expression of the *ChP*. They find the recurrence relations among its coefficients. Later, they found that the sum of the coefficients for cyclo-para-phenylene graphs model physical properties, such as the strain energy and diameter of CPPs [202,203].

Gutman postulated a relation that holds for trees between the *ChP* and the Hosoya index Z [204]. Later, Cash extended it to (poly)cyclic graphs by substituting the matching polynomial for the *ChP* [205].

The *ChP* is related to the Laplacian polynomial, which is discussed later [197]. Other modifications of the *ChP* have been put forward, such as the μ -polynomial and the β -polynomial [149].

The *ChP* admits extensions. The Hückel's method of molecular orbital is the first of these. The "secular determinant" is the determinant of a matrix that is decomposed as $|E \cdot Id - Ad|$ (the energy of the system "E" instead of x). He uses this form to approximate treatment of π electron systems in organic molecules. Hartree and Fock had another direction and ended up with the second extension by approximating treatment of the wave function. It was the same older eigenvector–eigenvalue problem in Slater's treatment of molecular orbitals. An extension was pursued with the ability to explain area and volume [197].

Since the *ChP* is related to the Hosoya polynomial, it must also be related to the matching polynomial—both are defined by counting independent edges [197]. Among the plethora of other known results, some are stated by Diudea and reveal further deep lying analogies between the characteristic and the matching polynomials. The fundamental difference between *ChP* and *MP* is in the effect of cycles [149].

ChP might be thought of as the determinantal polynomial. One could also construct a permanent polynomial π as the permanent of $(x \cdot [Id] - [Ad])$ [206].

IV.2. Extending the characteristic polynomial²

The term "secular function" has been used for what is now called a characteristic polynomial (ChP, in some of the literature, the term secular function is still used). The ChP was used to calculate secular perturbations (on a time scale of a century, i.e., slow compared with annual motion) of planetary orbits [221]. The first use of the ChP ($|\lambda \cdot Id - Ad|$, where Id is the identity matrix, and Ad is the adjacency matrix) in relation with chemical structure appeared after the discovery of wave-based treatment at the microscopic level [222]. The Hückel's method of molecular orbitals is actually the first extension of the ChP definition. He uses the 'secular determinant'—the determinant of a matrix which is decomposed as

² Joița, D.-M.; Jäntschi, L. [197].

$|E \cdot \text{Id} - \text{Ad}|$, standing with the energy of the system (E instead of λ)—to approximate treatment of π electron systems in organic molecules [222].

The second extension of the ChP was found by Hartree [223,224] and Fock [225,226] by going in a different direction with the approximation of the wave function treatment. They actually found the same older eigenvector–eigenvalue problem (§20 in [227]; T1 in [228]) in Slater’s treatment [229,230] of molecular orbitals. More generally (and older), the eigen-problem (finding of eigenvalues and eigenvectors) is involved in any Hessian [231] matrix $[A]$ ($[\text{Ad}] \rightarrow [A]$, where Ad is the adjacency matrix). The Laplacian polynomial is a polynomial connected with the ChP (in Table IV.2.1). This uses a modified form (the Laplacian matrix, $[\text{La}]$) of the adjacency matrix ($[\text{Ad}]$), $[\text{La}] = [\text{Dg}] - [\text{Ad}]$, where $[\text{Dg}]$ simply counts on the main diagonal the number of the atom’s bonds (the rest of its elements are null; for convenience with the graph-theory-related concept, it was denoted $[\text{Dg}]$, from vertex degree). The ChP is related also to the matching polynomial [232], degenerating to the same expression for forests (disjoint union of trees). Adapting [233] for molecules, a k -matching in a molecule is a matching with exactly k bonds between different atoms; see §3.1 & §3.3 in [149] for details. Each set containing a single edge is also an independent edge set; the empty set should be treated as an independent edge set with zero edges—this set is unique due to the constraint of connecting different atoms, where the matching may involve no more than $\lfloor n/2 \rfloor$ bonds, where n is the number of atoms. It is possible to count the k -matches [234], but, nevertheless, it is a hard problem [235], as well as to express the derived Z-counting polynomial [108] and matching polynomial—both are defined using $m(k)$ as the k -matching number of the selected molecule, as shown in Table IV.2.1 (where n is the number of atoms).

Name	Formula
ChP	$ \lambda \cdot [\text{Id}] - [\text{Ad}] $
LaP	$ \lambda \cdot [\text{Id}] - [\text{Dg}] + [\text{Ad}] $
Z-counting	$\sum_{k \geq 0} m(k) \cdot \lambda^k$
Matching	$\sum_{k \geq 0} (-1)^k \cdot m(k) \cdot \lambda^{n-2k}$

Table IV.2.1 Characteristic polynomial (ChP), Laplacian polynomial (LaP), Z-counting, and Matching Polynomials.

A topological description of a molecule requires the storing of the bonds (as adjacencies) between the atoms and the atoms themselves (as identities). If this problem is simplified at maximum, by disregarding the atom and bond types, then the molecule is seen as an undirected and unweighted graph. The graph structure can be translated into the informational space by numbering the atoms. Unfortunately, this procedure also induces an isomorphism—the isomorphism of numbering, which may collapse into a nondeterministic polynomial time to be solved [236]. This is a reason for the desire of graph invariants, e.g., which do not depend on the numbering made on the graph.

Once the atoms (or the vertices) are numbered, the information can be simply stored as lists of vertices (V) and edges (E), and the graph structure of the molecule is associated with the pair $G = (V, E)$. An equivalent representation is obtained using matrices. The adjacencies ($[Ad]$) are simply stored with 0 when no bond connects the atoms and 1 when a bond connecting the atoms exists. The identity matrix ($[Id]$) identifies the atoms by placing 1 on the main diagonal and 0 otherwise.

The ChP is the natural construction of a polynomial (in λ) in which the eigenvalues of $[Ad]$ are the roots of the ChP as follows:

λ is an eigenvalue of $[Ad] \rightarrow$ there exists an eigenvector $[v] \neq 0$ such that $\lambda \cdot [v] = [Ad] \times [v]$.

As a consequence $(\lambda \cdot [Id] - [Ad]) \cdot [v] = 0$.

Since $[v] \neq 0 \Rightarrow \lambda \cdot [Id] - [Ad]$ is singular; $\Rightarrow |\lambda \cdot [Id] - [Ad]| = 0$.

Finally, as seen in equation (4),

$$ChP \leftarrow |\lambda \cdot [Id] - [Ad]| \quad (4)$$

ChP is a polynomial (in λ) of degree n , where n is the number of atoms. The ChP finds its uses in the topological theory of aromaticity [237,238], structure-resonance theory [239], quantum chemistry [240], and counts of random walks [241], as well as in eigenvector–eigenvalue problems [242].

This definition allows extensions. A natural extension is to store in the identity matrix ($[Id]$) non-unity instead of unity values ($[Id]_{ij} = 1 \rightarrow [Id]_{ij} \neq 1$) accounting for the atom types, as well as to store in the adjacency matrix ($[Ad]$) non-unity instead of unity values accounting for the bond types ($[Ad]_{ij} = 1 \rightarrow [Ad]_{ij} \neq 1$). This extension was subjected to study in the context of deriving structural descriptors useful for structure–property relationships.

The topology of a graph structure could be expressed as matrices, and, in this regard, three of them are more frequently used: identity, adjacency (vertex–vertex, edge–edge, and vertex–edge), and distance matrices can be built (Table IV.2.2).

Definition	V: Finite Set	$E \subseteq V \times V$	$G = G(V,E)$
Name (concept)	V: vertices (atoms)	E: edges (bonds)	G: graph (molecule)
Cardinality	$ V = n$	$ E = m$	$\forall n, V \leftrightarrow \{1, \dots, n\}$
Example	$G = \text{"A-B-C"}$	$V = \{1,2,3\}$	$E = \{(1,2), (2,3)\}$

Table IV.2.2 Classical molecular graphs.

The matrices reflect in a 1:1 fashion the graph if the full graph is stored (each vertex pair stored twice, in both ways). The matrices of vertex adjacency ($[Ad]$) and of edge adjacency are square and the double enumeration of the edges is reflected in symmetry relative to the main diagonal (see Figure IV.2.1).

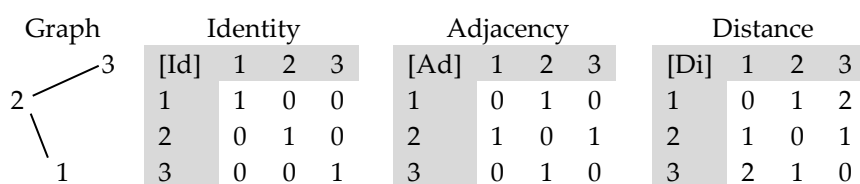


Figure IV.2.1 Encoded identities $[I]$, adjacencies $[A]$ and distances $[D]$ —an example.

ChP is the natural construction of a polynomial in which the eigenvalues of the [Ad] are the roots of the ChP. ChP is a polynomial in λ of degree n , where n is the number of atoms. A natural extension is to store in [Id] (instead of unity) non-unity values accounting for the atom types, as well as to store in [Ad] (instead of unity) non-unity values accounting for the bond types.

An extremely important problem in chemistry is to uniquely identify a chemical compound. If the visual identification (looking at the structure) seems simple, for compounds of large size, this alternative is no longer viable. The data related to the structure of the compounds stored into the informational space may provide the answer to this problem. Nevertheless, together with the storing of the structure of the compound another issue is raised—namely, the arbitrary numbering of the atoms (Figure IV.2.2).

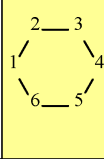
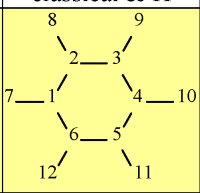
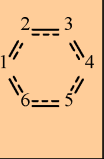
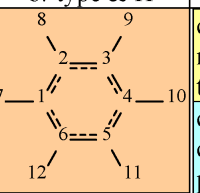
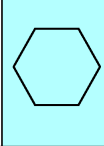
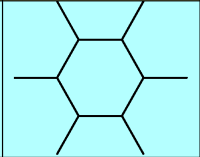
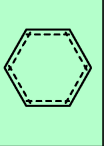
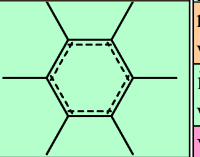
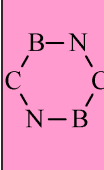
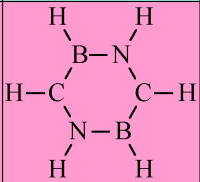
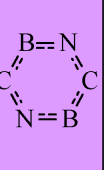
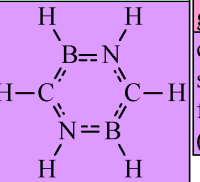
&	classical	classical & H	b.-type	b.-type & H	groups
num.					classical molecular topology
un-num.					numbered weighted graphs isomorphic-free weighted graphs
a.-type					vertex-labeled graphs chemical structural formula (labeled graphs)

Figure IV.2.2 Graphs vs molecules—an example.

For a chemical structure with N atoms stored as a (classical molecular) graph, there exist exactly $N!$ possibilities for numbering the atoms. Unfortunately, storing the graphs as lists of edges and (eventually) vertices does not provide a direct tool to check this arbitrary differentiation due to the numbering. The same situation applies to the adjacency matrices. Therefore, seeking for graph invariants is perfectly justified: an invariant (graph invariant) does not depend on numbering. The adjacency matrix is not a graph invariant and, therefore, it is necessary to go further than the adjacencies.

Important classes of graph invariants are the graph polynomials. To this category belongs the ChP—a graph invariant encoding important properties of the graph. On the other hand, unfortunately, ChP does not represent a bijective image of the graph, as there exist different graphs with the same ChP (i.e., cospectral graphs—the smallest cospectral graphs occurs for 5 vertices [243]). In order to count the cospectral graphs, one should compare A000088 and A082104 [244,245]. The ideal situation is that the invariant should be uniquely assigned to each structure, but this kind of invariant is difficult to find. A proce-

ture to generate a non-degenerate invariant proposed by IUPAC is the international chemical identifier (InChI), which converts the chemical structure to a table of connectivity expressed as a unique and predictable series of characters [246].

Despite this inconvenience (not representing a bijective image of the graph) due to its link with the partition of the energy [222], the ChP seems to be one of the best alternatives for quantifying the information from the chemical structure.

Previously, researchers have shown the performance of estimation and/or prediction of the ChP on nonane isomers [178,247,248] as well as in the case of carbon nanostructures [249,250]. Furthermore, an online environment has been developed to assist researchers in the calculation of polynomials based on different approaches; including ChP [251].

When doing calculations on molecular graphs, it is important to consider that, with the increase in the simplification in the graph representation (such as neglecting the type of the atom, bond orders, geometry in the favour of topology), the degeneration of the whole pool of possible calculations increases and there are more molecules with the same representation. This is favourable for the problems seeking similarities but is clearly unfavourable for the problems seeking dissimilarities.

A necessary step to accomplish better coverage of similarity vs dissimilarity dualism is to build and use a family of molecular descriptors, large enough to be able to provide answers for all. In the natural way, such a family should possess a ‘genetic code’—namely, a series of variables from which to (re)produce a (one by one) molecular descriptor, all descriptors being therefore obtained in the same way. It is expected that all individuals of the family are independent of the numbering of the atoms in the molecule (should be molecular invariants).

The construction of such a family needs to consider the following:

- Molecules carry both topological and geometrical features (see Figure IV.2.3);
- Atom and bond types are essential factors in the expression of the measurable properties;
- Atom and/or bond numbering induces an undesired isomorphism;
- Geometry and bond types induce other kinds of isomorphism.

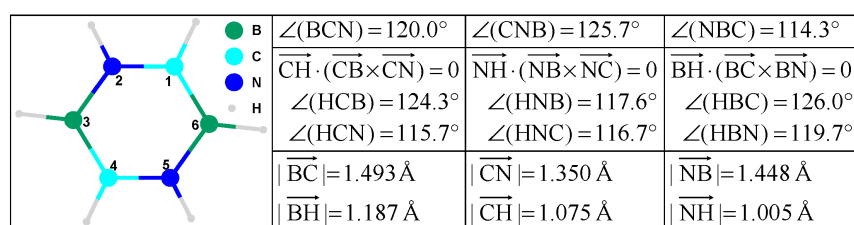


Figure IV.2.3 Molecular geometry—an example.

The representation of a molecule could be done using identity and adjacency as presented in Figure IV.2.4.

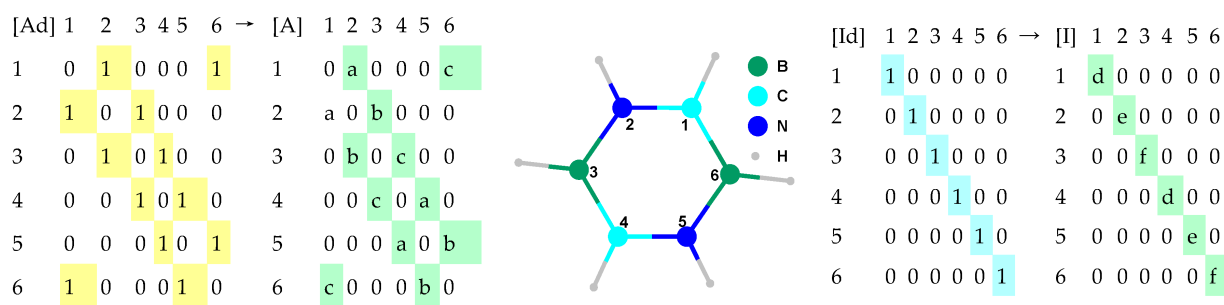


Figure IV.2.4 Molecular geometry translated into adjacency and identity—an example.

The distinct identities from Figure IV.2.4 are given using *a*, *b*, and *c* as variables in the case of adjacency and using *d*, *e*, and *f* as variables in the case of identity. This formalism allows the introduction of a natural extension of the ChP from graphs to molecules. There is no determinism in selecting the values of *a*–*f*. However,

- If $a = b = c = d = e = f = 1$ then $\text{ChPE} \leftarrow \text{ChP}$ as in classical molecular topology.
- If $a = b = c = 1.5-1$, then $[A]$ accounts for the (inverse of the) bond order.
- If $a = 1.35-1$, $b = 1.448-1$, and $c = 1.493-1$ then $[A]$ accounts for the (inverse of the) geometrical distance (in Å).
- If $d = 12/294$, $e = 14/294$, and $f = 10.8/294$, then $[I]$ accounts for atomic mass relative to Uuo, the last element from the 7th period of the system of elements.
- If $d = 2267/\rho_{\text{ref}}$, $e = 1026/\rho_{\text{ref}}$, and $f = 2460/\rho_{\text{ref}}$, then $[I]$ accounts for the solid state relative density (in m^3/kg); ρ_{ref} can be fixed to 30,000.
- If $d = 2.55/4.00$, $e = 3.04/4.00$, and $f = 2.04/4.00$, then $[I]$ accounts for electronegativity relative to Fluorine when the Pauling scale is used.
- If $d = 1086.2/1312$, $e = 1402.3/1312$, and $f = 800.6/1312$, then $[I]$ accounts for the first potential of ionization relative to the potential of ionization for Hydrogen.
- If $d = 3820/3820$, $e = 63/3820$, and $f = 2573/3820$, then $[I]$ accounts for melting point relative to the diamond allotrope of Carbon (in K).
- If $d = 1/4$, $e = 1/4$, and $f = 1/4$, then $[I]$ accounts for the number of hydrogen atoms attached relative to the score of CH_4 .

The full extension could include also the distance matrix (Figure IV.2.5).

[Ad]	1	2	3	4	5	6	→	[Id]	1	2	3	4	5	6	→	[Di]	1	2	3	4	5	6	→	[I]	1	2	3	4	5	6	
1	0	1	0	0	0	1		1	1	0	0	0	0	0		1	1	0	0	0	0	0		1	d	0	0	0	0	0	
2	1	0	1	0	0	0		2	0	1	0	0	0	0		2	0	1	0	0	0	0		2	0	e	0	0	0	0	
3	0	1	0	1	0	0		3	0	0	1	0	0	0		3	0	0	1	0	0	0		3	0	0	f	0	0	0	
4	0	0	1	0	1	0		4	0	0	0	1	0	0		4	0	0	0	1	0	0		4	0	0	0	d	0	0	
5	0	0	0	1	0	1		5	0	0	0	0	1	0		5	0	0	0	0	1	0		5	0	0	0	0	e	0	
6	1	0	0	0	1	0		6	0	0	0	0	0	1		6	0	0	0	0	0	1		6	0	0	0	0	0	f	
↓ extension ↓														↓ extension ↓																	
[A]	1	2	3	4	5	6	→	[I]	1	2	3	4	5	6	→	[D]	1	2	3	4	5	6	→	[I]	1	2	3	4	5	6	
1	0	a	0	0	0	c		1	d	0	0	0	0	0		1	0	a	h	k	g	c		1	d	0	0	0	0	0	
2	a	0	b	0	0	0		2	0	e	0	0	0	0		2	0	a	0	b	g	j	i		2	0	e	0	0	0	0
3	0	b	0	c	0	0		3	0	0	f	0	0	0		3	0	0	0	c	i	l		3	0	0	0	f	0	0	0
4	0	0	c	0	a	0		4	0	0	0	d	0	0		4	0	0	0	0	a	h		4	0	0	0	0	d	0	0
5	0	0	0	a	0	b		5	0	0	0	0	e	0		5	0	0	0	0	0	a	b		5	0	0	0	0	e	0
6	c	0	0	0	0	b		6	0	0	0	0	0	f		6	0	0	0	0	0	0		6	0	0	0	0	0	f	

Figure IV.2.5 Molecular geometry translated into adjacency, identity, and distance—an example.

The extended ChP has the following formula:

$$\text{ChP} \leftarrow |\lambda \times [\text{I}] - [\text{C}]| ,$$

where [C] is either [A] or [D], the identities (a, b, and c from [I]) and the connectivity (d, e, f, g, h, i, j, k, and l from [C]).

The single-value entries (0 and 1 \neq 0 for the classical definition of the ChP) can be upgraded to multi-value (any value), accounting for different atoms and bonds. Obviously, the classical ChP is found when $a = b = c = d = e = f = 1$ and $g = h = i = j = k = l = 0$.

EChP is a family with 96 ($n\text{I} \times n\text{C}$) polynomial formulas and 288 ($*n\text{L}$) linearized ones, leading to a total of 576,288 individuals. The FreePascal software was used for implementation since it is very fast and allows a parallelized version to be used with multi-CPUs (chp17chp.pas) [252]. The program requires input files in the "chp" format (such as chfp_17_q.asc, see Figure IV.2.7), and uses a filtering (PHP) program (\rightarrow chfp_17_t.asc) as well as a molecular property file (such as chfp_17 [prop].txt). The filtering program was designed to look for degenerations and to reduce the pool of descriptors by eliminating the degenerated ones.

The family of EChP descriptors was then used with a series of chemical compounds to obtain associations between the structure and properties as regression equations.

The case study was conducted on C_{20} fullerene congeners with Boron, Carbon, or Nitrogen atoms on each layer (Figure IV.2.8). A sample of 45 distinct compounds was obtained. The generic name of the files was stored as dd_R1R2R3R4, where dd is the number of the compound in the set and R1–R4 are the atoms on layers 1–4 (e.g., 02_bbbn.chp is the second compound in the sample and has boron on the first three layers and nitrogen on the last layer).

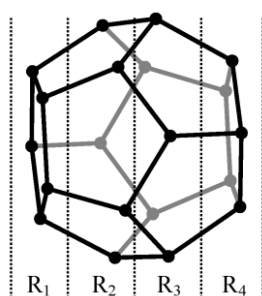


Figure IV.2.8 C_{20} fullerene congeners (R is the symbol of the atom on the layer).

The geometries were built at the Hartree-Fock (HF) [223–226] 6-31 G [253] level of theory and calculated properties (namely, area and volume) were extracted from these calculations. Two different structures proved stable for bbbb (see Figure IV.2.9) and both were included in the analysis, resulting in a sample of 46 compounds.

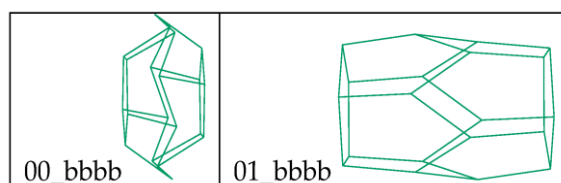


Figure IV.2.9 bbbb C₂₀ stable fullerenes.

The values of the calculated properties are given in Table IV.2.3.

Mol	Area	Volume	Mol	Area	Volume	Mol	Area	Volume
00_bbbb	54.641	30.063	16_cbbb	50.537	27.863	31_ccnc	42.689	22.542
01_bbbb	51.863	26.948	17_cbbc	51.114	29.107	32_ccnn	43.987	23.862
02_bbbn	54.848	32.333	18_cbbn	49.097	27.424	33_cnbb	49.186	28.569
03_bbcn	48.481	27.524	19_cbc b	51.733	30.156	34_cnb n	44.694	24.794
04_bbnb	53.093	30.658	20_cbc n	47.401	26.543	35_cnc b	46.994	26.275
05_bbn n	49.797	27.573	21_cbn b	48.262	26.68	36_cnc n	44.723	24.062
06_bcb b	54.597	32.043	22_cbnc	45.944	25.109	37_cnn b	45.76	24.995
07_bcb n	49.415	28.726	23_cbnn	45.578	24.689	38_cnnc	48.834	24.315
08_bccb	51.676	29.739	24_ccbb	52.365	30.954	39_cnn n	45.508	24.847
09_bcc n	47.392	26.933	25_ccbc	45.618	24.718	40_nbb n	48.119	26.881
10_bcn b	48.782	26.786	26_ccbn	45.857	25.514	41_nbn n	45.726	24.275
11_bcnn	47.15	25.543	27_cccb	46.446	25.49	42_ncb n	45.735	25.533
12_bnb n	47.791	27.383	28_cccc	43.707	23.584	43_ncc n	45.211	24.676
13_bnc n	47.048	26.368	29_cccn	43.86	23.926	44_ncn n	44.848	24.445
14_bnn b	48.244	27.25	30_ccnb	45.901	25.525	45_nnn n	46.463	25.872
15_bnn n	47.226	25.93	-	-	-	-	-	-

Table IV.2.3 C₂₀ congeners: values of investigated properties.

It is important that the performing models identified using the EChP descriptors—the full model—select the same polynomial for both descriptors when both area and volume are investigated. It should be noted that one descriptor is common for the estimation of the area and of the volume for the C₂₀ fullerene congeners. This fact, in conjunction with the higher correlation between volume and area ($r^2_{\text{adj}} \approx 0.97$), the presence of outliers in one additive model, and the significant higher performance by full models in estimation sustained by goodness-of-fit and the graphical representation of calculated versus estimated, suggests that the best models are those with full effects.

EChP proved useful for estimation of the investigated molecular properties. Both properties of C₂₀ congeners—volume and area—are explained by a common descriptor. EChP is a natural extension of the ChP. The scales of the atomic properties were more or less arbitrary selected and will be further investigated to find the optimal solution. Furthermore, the reversed distance seemed to be the best alternative but further analysis must be conducted to demonstrate this observation.

IV.4. An application of the eigenproblem³

Just visualizing two simple similar structures leads to an immediate detection of patterns. Similarity is of convenience for humans, but in order to power automatic decision mechanisms for a PC it must be measurable. It is mostly used for comparing proteins but the growing number of PDB structures is many orders of magnitude higher than what the human eye can compare. Battery databases are also coming from behind, one of which containing over 17000 unique chemicals [262,263]. Because of the large number, it takes days even for some programs to search some databases for a query structure. A more reasonable time can be achieved by developing new algorithms [264].

In a previous study the eigenproblem was employed to achieve the proper alignment, or the mirror of the proper alignment, and this can be exploited to reduce the number of rotations for which a scoring function needs to run [276].

The eigenproblem is thus defined in literature:

Given the quadratic matrix A , of the order n , $\lambda \in \mathbb{C}$ is called the eigenvalue of the matrix A and $X \neq 0$ its associated eigenvector if the relationship is satisfied $AX = \lambda X$. The matrix $\lambda I - A$ is singular (because $\det(\lambda I - A) = 0$), where I is the unit matrix of order n . The solutions of the equation $\det(\lambda I - A) = 0$ represent the eigenvalues of the matrix A .

The development of the determinant $\det(\lambda I - A)$ is called the characteristic polynomial (ChP) associated with matrix A . It has the degree equal to the order of the matrix, so that the eigenvalues of the matrix A are its roots.

The eigenproblem in relation to geometrical alignment was stated before in the context of surface analysis [277] and control and can go another direction into the context of compounds used in energy storage systems. A subject of the study is a solution to the eigenproblem of such compounds that are aligned. The Cartesian system is rotated, and eventually translated and reflected until the structure arrives in a position characterized by the highest absolute values of the eigenvalues observed on the Cartesian coordinates.

The aim of this study is to find the best alignment of many compounds in regards to each-other. An extension to the previous study described by Jäntschi [276] was elaborated. Similar candidates are found by comparing sums of squared eigenvalues. Candidates are aligned by the eigenproblem algorithm and trilateration is used to attach all previously striped atoms. In order to verify, TM-score is run on resulting full-structure candidates.

In [276] it has been shown that the Cartesian distance matrix is antisymmetric and therefore its eigenvalues are purely imaginary, as well as the fact that the best alignment of a molecule is obtained for the minimum value of the sum of the squares of the eigenvalues of the matrix of Cartesian distances.

Thus, the angle of rotation of the structure must be found around an axis for which the minimum of this amount is obtained. One method of finding the angle of rotation

³ Joița, D.-M.; Tomescu, M.A.; Bălint, D.; Jäntschi, L. [261].

around an axis for best alignment is as follows: in the case of a compound with 5 atoms, we will note the vertices of the graph corresponding to the compound with $V_i(x_i, y_i, z_i)$, $i = \overline{1,5}$. We want to find the optimal angle of rotation around the Oz axis (for example). The characteristic polynomial associated with the matrix of Cartesian distances on Ox can be approximated in this way:

$$ChP(\lambda, Dx) = \lambda^3 \left[\lambda^2 + \sum_{\substack{j=1 \\ i=j+1}}^{n-1} (x_i - x_j)^2 \right],$$

which leads to the problem of finding the rotation angle in the xOy plane so as to obtain the maximum value of the sum:

$$S_x = \sum_{\substack{j=1 \\ i=j+1}}^{n-1} (x_i - x_j)^2.$$

Because the term $(x_i - x_j)^2$ becomes maximum when $\sphericalangle(V_j V_i, Ox) = 0$, we will calculate the amount S_x using the law of motion of the rotation of a body about a fixed axis:

$$\begin{cases} x'_i = x_i \cos \varphi - y_i \sin \varphi \\ y'_i = x_i \sin \varphi + y_i \cos \varphi \end{cases}$$

where φ will take the value in turn $\sphericalangle(V_j V_i, Ox)$; $j = \overline{1, n-1}$; $i = j + 1$.

By interpolation, we will find the value of the angle of rotation around the Oz axis, and around one of the other axes. The eigenvalues of the associated Cartesian coordinate distance matrix Dx are always two conjugate purely imaginary solutions: $\lambda_1^2 = \lambda_2^2 = -S_x$.

Sums of the form $S_T = -2S_x - 2S_y - 2S_z$, associated with Dx, Dy, and Dz matrices, are compared in order to find similarities. One application of this approach can start by finding ChP for Cartesian coordinate distance matrices. These are used to define minima of the sums of the squared eigenvalues (S_x , S_y and S_z) for these matrices.

The following three Tables IV.4.1-3 depict the approximated Cartesian coordinate distance matrices for atoms of SrTiO₃ 5229. They are antisymmetric so their eigenvalues, in Table IV.4.4, will be imaginary.

Dx	1	2	3	4	5
1	0	0.00009	-1.38326	-0.000003	1.38344
2	-0.00009	0	-1.38335	-0.00009	1.38335
3	1.38326	1.38335	0	1.38326	2.7667
4	0.000003	0.00009	-1.38326	0	1.38344
5	-1.38344	-1.38335	-2.7667	-1.38344	0

Table IV.4.1 First Cartesian coordinate (“x”) distances matrix for SrTiO₃ 5229.

	x ₁	x ₂	x ₃	x ₄	x ₅
[Dx]	4.37453i	-4.37453i	0	0	0
[Dy]	4.37453i	-4.37453i	0	0	0
[Dz]	5.5334i	-5.5334i	0	0	0

Table IV.4.4 Eigenvalues for SrTiO₃ 5229.

1	-307.5042	4	-206.3409	7	-290.7693	10	-206.3411	13	-189.0737	16	-225.5829	19	-193.1574
2	-261.1036	5	-242.4953	8	-261.1036	11	-336.4603	14	-225.5830	17	-189.0739	20	-267.8521
3	-290.7693	6	-336.4603	9	-242.4951	12	-259.1272	15	-319.3706	18	-319.3706	21	-267.8523

Table IV.4.6 Eigenvalue sums of 21 combinations of 5 atoms for Ta₂O₅ 1238961.

S _x + S _y + S _z		S _x + S _y + S _z		S _x + S _y + S _z		S _x + S _y + S _z		S _x + S _y + S _z		S _x + S _y + S _z		S _x + S _y + S _z	
1	-194.5721	6	-171.1067	11	-137.5761	16	-171.1067	21	-71.75625	26	-113.9332	31	-177.3704
2	-194.5721	7	-71.75610	12	-231.1220	17	-137.5760	22	-201.4564	27	-113.9333	32	-103.0947
3	-146.6665	8	-144.4196	13	-112.3626	18	-137.9311	23	-112.3626	28	-207.3018	33	-177.3704
4	-146.6667	9	-201.4564	14	-150.3065	19	-231.1220	24	-186.4607	29	-103.0947	34	-140.8613
5	-240.0351	10	-137.9309	15	-186.4609	20	-144.4195	25	-150.3067	30	-140.8612	35	-148.5577

Table IV.4.7 Eigenvalue sums of combinations of 4 atoms for Ta₂O₅ 1238961.

S _x + S _y + S _z	
1	-68.8915
2	-91.8553
3	-84.2007
4	-84.2007
5	-84.2007

Table IV.4.8 Eigenvalue sums of combinations of 4 atoms for SrTiO₃ 5229.

The “moreData” function parses every potential candidate to find good candidates, with the lowest difference between S_x + S_y + S_z sums in mind. “Num.low” defines the desired % difference. The multiplier “Num.M” is selected to increase the search range at the expense of time because the best candidate may not always be the one with the smallest difference between sums. In this case we can see in Tables IV.4.6-8 that the sums of 5 atom combinations coloured in blue of Ta₂O₅ 1238961 are far from the eigenvalue sum of SrTiO₃ 5229; there are two possibilities with closer sums for 4 atom combinations coloured in orange; and two coloured in red that are the closest. This aspect is presented in Table IV.4.9:

Ta ₂ O ₅ 1238961				Difference		SrTiO ₃ 5229								
atoms				sum	%	sum	atoms							
-	Ta2	-	O4	-	O6	O7	-71.7561	3.9921	-68.8915	-	Ti2	O3	O4	O5
Ta1	-	O3	-	O5	-	O7	-71.7563	3.9923	-68.8915	-	Ti2	O3	O4	O5
Ta1	Ta2	-	O4	-	-	O7	-103.0947	10.9020	-91.8553	Sr1	-	O3	O4	O5
Ta1	Ta2	O3	-	-	-	O7	-103.0947	10.9020	-91.8553	Sr1	-	O3	O4	O5
Ta1	Ta2	-	O4	-	O6	O7	-189.0737	27.1268	-137.7840	Sr1	Ti2	O3	O4	O5
Ta1	Ta2	O3	-	O5	-	O7	-189.0739	27.1269	-137.7840	Sr1	Ti2	O3	O4	O5

Table IV.4.9 Selected atoms of aligned Ta₂O₅ 1238961 to SrTiO₃ 5229, eigenvalue sums of candidates, and eigenvalue sums percent difference.

In Table IV.4.9 it can be observed that a difference exists at the 4th digit after the decimal point. For this reason four digits will be used after the decimal point in all tables for results of geometrical similarities. On the selected candidates, the eigenproblem technique is applied to obtain an eigen-value-wise rotation alignment. Compounds are supposed to be obtained in the mirror image of the proper alignment or in their correct alignment [276]. By using the first “for” instruction of the “align” function, the search is expanded to include these potential favourable rotations. A trilateration procedure (receiving data from the rest

of the “align” function) is found and used from literature to determine the position of the other mismatched, unaligned atoms [278].

Since one of these rotations should lead to a good superposition of the two compounds, the mean values on each of the axes are found for selected atoms of both structures. The selection is based on atoms indexed in the candidate search presented in Table IV.4.9. Subtracting for each of the axes, the candidate structure is translated on top of SrTiO₃ 5229 (by the “trans” function).

Distances between pairings of multiple atoms are found for the resulting candidate combinations. Atoms that will be super-posed based on a linear assignment problem that permits minimum-cost solutions are found using the “matchpairs” Matlab function. These pairs are fed into a scoring system that is selected from the literature; in this example, it's the UniAlign - TMscore geometric component [279]. This is all carried out by the “choice” function. Since there aren't many atoms in the structures we've picked, one adjustment: we adjusted was made, the “15” subtraction is changed to zero in order to get a positive distance under the square root of the empirical scaling factor for distance normalisation, or “d0”. This is modifiable in “empi3”. Additional scoring mechanisms could be utilised. The best result is superposed in Figure IV.4.2.

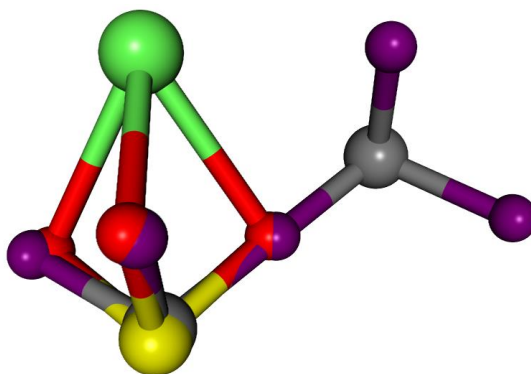


Figure IV.4.2. 3D view of the best alignment of Ta₂O₅ 1238961 (Ta grey; O purple) to SrTiO₃ 5229 (Sr green; Ti yellow; O red).

Each comparison structure's best score is exported to a final results table. Scores that are near it are added using the “Num.low2” parameter. The table displays the elements that were chosen for candidate-candidate alignment because they facilitate selecting between scores that are near to each other. An “*Tscore.xls” file is produced upon completion of the “choice” function.

Discussion

The eigenproblem algorithm's best match can be chosen from among all the candidates by using TM-score. In the published article amino-acids were aligned, and in this thesis, compounds used in energy storage systems are aligned and presented.

As previously mentioned, a parameter is included to ensure that close scores are taken into account. In this instance, an output score of 80% of the maximum is allowed. “Num.low2” changes this proportion. This is necessary to ensure that, even if it isn't the alignment with the greatest TM-score, the best alignment is included in the output.

Examining the selected elements and removing contenders that may have similar numerical scores but the incorrect element. The elements are shown to easily select from these options. Even better outcomes could be achieved by using a mix of these methods or alternative scoring systems.

The application and utilisation of eigenproblem extends beyond molecular alignment [276] and biological similarity, including regular graphs analysis for their properties, including eigen-spectra and auto-morphisms [280], molecular topology [219,281–283], characteristic equations [284], principal components decomposition [285], algebraic topology and generalized Bertrand curves [286], treatment of fuzzy decision [287] and tridiagonal matrices [288], commutator tables [289], Laplacian [290], systems of differential [291] and integro-differential [292] equations, while challenging problems appears in polynomials roots evaluation [293] and characteristic equation of a square matrix of a great order [294].

It might be noted that the optimal alignment defies rigorous trends. It is possible to consider the same algorithm's close similarity results. We can conclude that the alignment with the greatest score is not always the optimum alignment from a chemical point of view, even after using an evaluation system. The current algorithm must be limited by a few parameters in order to decrease the number of rotations that a scoring function must perform. Additionally, combining several strategies may provide outcomes more quickly. A comprehensive database would demonstrate a rational process for selecting them.

In order to mitigate the effects of fixed theory-inspired functional form and restricted description capabilities, machine learning must be incorporated into scoring functions. These flaws can be fixed by allowing machine learning to capture properties that are difficult to predict due to numerous unmeasured, unknown, or undiscovered Quantitative Structure–Activity Relationships (QSAR), rather than enforcing a rigid approach. The rapidly increasing amount of high-quality structural and interaction data available in the literature can be assimilated using machine learning.

Improvements of the code

The main problem of the code from 2021 was that arrays were not pre-allocated. This meant that the program had to increase the size of the array for each step in the “for” loops. Since there are many possible combinatorial possibilities, this was the major issue slowing down results generation. One way of pre-allocating is starting the loop from the final step (example: for i = 300 : -1 : 1 ...).

Another improvement is vectorisation of the code (revising loop-based, scalar-oriented code to use Matlab matrix and vector operations). This improvement also relieves the above issue of pre-allocating array size.

A way of recursing all compounds automatically was added as the “for ka” loop.

Performance

Taking our case for example, comparing one compound to 293 files and up to 15 atoms per file, results in a 5 hour computer time spent. The final version is 180 faster than the published one. The writing of this thesis began when a timeframe of months was achieved through vectorisation of the code. Adding just one file containing 16 atoms increases computer time by at least 6 hours. In case similarities are found between compounds, more geometries can be downloaded for further comparison.

Further results of similarities

The first compounds are chosen parameters from an auto-generated database promising reliable parameters. Unfortunately it was not the case, and such parameters are no longer presented. Other compounds are chosen so that they relate to previous published articles presented above. The rest are chosen in bulk and this effort is on-going. Because of the large quantity of data, Cartesian information retrieval is stopped at 293 candidates. It is important to understand what can be done with such data, and to share for further insights before the on-going effort is continued.

After visualizing the possibilities, a “best” similar orientation for all combinations of two candidates is chosen. Normally, a higher score is given to candidates with more close atoms, but another orientation may seem better to the naked eye. This is noted such that subjectivity is taken into account.

The program gives tens of thousands of results in some cases from which those with the best score are chosen. Many of these have a low score and will be disregarded in the next step. Parameters are extracted from a database. Visual examples of good scores and similar parameters (energy above Hull, band gap, predicted formation energy) are presented. Those that present only a similar line or plane, and those with the same or similar space group are indicated as possible unavoidable results – coincidences. Table IV.4.10 presents examples of the best scores found by our program and similarities between Ca₂Si 1009733 and other candidates. The full version of the table is available in Appendix F.

After visualizing these alignments, a decision is made to disregard scores lower than 0.85 and candidates with three matched atoms and less. The most relevant results to chemistry are near the 0.9 TM-score and above 4 matched atoms. From the total of 293 initial candidates [295–490], we now take into account 73. Trying to further refine the findings, some observations are made that some similarities can be deduced from space group information with no need for complicated comparison, that a line or plane may be similar by

pure coincidence, that atoms seem far apart regardless of the score. Parameters are searched for in “The Materials Project” database. Data from the first four columns is used to find other similarities and evaluate geometrical similarities found by our program. At the end of displayed data a statistic will be present how these four columns aid similarities search. Table IV.4.11 presents these opinions and data.

Energy above Hull ^a eV/atom	Band gap ^a eV	Predicted formation energy ^a eV/atom	Space group (internal number) ^a	Aligned compound	TM-score	Number of atoms matched	Observations
0	0.55	-0.534	225	Ca ₂ Si 1009733			
0.037	0.06	-0.281	216	FeSiW 961653	0.8834	5	similar group
0	3.39	-1.525	225	Li ₂ S 1153	0.88658	12	same group
0	0.22	-0.109	225	Mg ₂ Si 1367	0.96168	12	same group
0.061	1.58	-1.759	166	MnO ₂ 25424	0.89772	4	line
0	1.2	-0.966	160	MoS ₂ 1434	0.92605	4	line
0.004	1.51	-0.961	187	MoS ₂ 1025874	0.97277	4	line
0.178	0	-0.393	160	Ni ₃ S ₂ 1220109	0.87572	5	line
2.223	0	1.432	216	SiCN 8003	0.88693	5	similar group
1.272	1.74	-1.774	225	SiO ₂ 10064	0.89502	5	same group
0.122	5.2	-2.924	1	SiO ₂ 556319	0.85746	5	far apart
0.423	2.75	-2.622	3	SiO ₂ 556376	0.86406	7	far apart
0.088	5.38	-2.958	1	SiO ₂ 556994	0.93605	4	far apart
0.005	5.5	-3.04	92	SiO ₂ 6945	0.89372	5	far apart
0.005	5.79	-3.041	96	SiO ₂ 7029	0.89578	4	far apart
0.005	5.79	-3.041	96	SiO ₂ 7029	0.86471	5	far apart
0.571	4.01	-2.474	205	SiO ₂ 9258	0.88541	5	far apart
0.799	0.39	-1.028	1	SiO ₄ 685105	0.85895	6	
0.015	0	-0.127	205	SiP ₂ 21065	0.86195	8	
0.017	0.96	-1.871	60	SnO ₂ 12978	0.85761	8	
0.162	2.1	-1.726	194	SnO ₂ 1041984	0.86931	4	far apart
0.246	0	-1.642	225	SnO ₂ 12979	0.85417	5	far apart
0.101	0.59	-1.787	205	SnO ₂ 697	0.93791	8	
0.278	0.17	-0.193	216	SnS 10013	0.93215	8	similar group
0.157	0	0.157	216	SnSb 16365	0.99597	8	similar group
0.252	0.08	-0.013	216	SnTe 16364	0.99984	8	similar group
0	5.23	-2.75	225	SrCl ₂ 23209	0.9983	12	same group
0	1.93	-2.263	14	TaNO 4165	0.87358	7	far apart
0	0	-1.38	160	Ta ₂ S ₂ 10014	0.92503	4	far apart
0	0	-0.7	194	Ti ₂ AlC 12990	0.88008	4	far apart
0.014	0	-0.629	166	Ti ₂ C 1217106	0.91731	4	far apart
0.05	0	-0.681	194	Ti ₃ C ₂ 1094034	0.89769	4	line
0.05	0	-0.681	194	Ti ₃ C ₂ 1094034	0.88785	5	line
0.002	0	-3.669	167	TiF ₃ 562468	0.86346	5	far apart
0.004	0	-0.53	225	TiH ₂ 24161	0.86808	5	far apart
0.7	0	0.171	216	TiNiSn 22782	0.94402	12	similar group
0.664	0	0.135	216	TiNiSn 623646	0.94296	12	similar group
0	0.45	-0.529	216	TiNiSn 924130	0.92494	8	similar group
0.25	1.38	-3.072	205	TiO ₂ 1102591	0.87957	6	far apart
0.25	1.38	-3.072	205	TiO ₂ 1102591	0.85096	11	far apart
0.005	2.53	-3.317	60	TiO ₂ 1439	0.89067	7	

Energy above Hull ^a eV/atom	Band gap ^a eV	Predicted formation energy ^a eV/atom	Space group (internal number) ^a	Aligned compound	TM-score	Number of atoms matched	Observations
0.01	2.89	-3.312	62	TiO ₂ 2420244	0.89492	6	
0.039	2.23	-3.283	14	TiO ₂ 430	0.87789	7	
0.526	1.7	-2.796	11	TiO ₂ 572822	0.85873	5	
0.046	1.93	-3.276	12	TiO ₂ 766454	0.87952	5	
0.302	1.06	-3.02	225	TiO ₂ 1008677	0.87666	5	far apart
0.302	1.06	-3.02	225	TiO ₂ 1008677	0.87665	5	far apart
0.153	2.45	-3.169	166	TiO ₂ 25433	0.92319	4	far apart
0.008	2.18	-3.314	15	TiO ₂ 34688	0.87535	7	
0.002	0	-1.605	164	TiS ₂ 1101258	0.91004	4	far apart
0.542	0	-0.799	160	TiS ₃ 559374	0.85056	5	far apart
0	0	-0.538	63	TiSi₂ 1077503	0.89161	5	
0.043	0	-2.477	14	VO ₂ 1102963	0.86704	6	
0.308	0	-2.212	166	VO ₂ 25199	0.90084	4	line
0.539	1.12	-1.981	10	VO ₂ 559445	0.88066	4	far apart
0.018	0	-1.182	166	VOF 753622	0.92477	7	
0.009	1.91	-2.489	2	VPO ₅ 1100906	0.86483	7	
0.022	1.42	-2.477	129	VPO ₅ 19000	0.85845	5	plane
0.018	0	-1.182	166	VS ₂ 1424931	0.93525	4	line
0.02	0	-2.212	65	VSbO ₄ 1100902	0.88819	7	
0.757	0.08	-0.574	160	WNO 1216189	0.93273	4	line
1.229	0	-0.959	194	WO ₃ 1386422	0.90472	4	line
0.001	1.6	-0.882	160	WS ₂ 9813	0.92598	4	line
0.059	0.11	-0.747	156	Zn(InS ₂) ₂ 22253	0.91211	4	line
0.085	3.27	-1.028	166	ZnBr ₂ 569960	0.96721	4	line
0.002	3.56	-2.561	60	ZnF ₂ 7709	0.85582	8	
0.141	1.8	-0.765	166	ZnI ₂ 570964	0.95341	4	line
0	1.07	-0.684	216	ZnTe 2176	0.85358	4	similar group
0.002	3.26	-2.052	13	ZnWO ₄ 18918	0.8773	7	
0.89	0	0.733	216	ZrCrFe 631429	0.91997	8	similar group
0.007	0	-0.63	225	ZrH ₂ 24155	0.88558	5	same group
0	3.53	-3.787	14	ZrO ₂ 2858	0.86592	7	far apart
0.029	2.99	-3.759	62	ZrO ₂ 755759	0.85039	5	line

^a Materials Data by Materials Project in references [25–40, 295–490].

Table IV.4.11 Data retrieved from “The Materials Project” database for Ca₂Si (material 1009733), similarity score, matched atoms and observations.

There are a few candidates that also share close predicted formation energy: TiNiSn 924130 (possible coincidence), TiSi₂ 1077503 (clearly not a coincidence) and ZrH₂ 24155 (coincidence). Of these, the first also has a band gap close to that of Ca₂Si 1009733. Two of them only have 5 matched atoms. As such, care should be taken not to eliminate candidates with a low number of matched atoms. Until now, relatively low scores show good results. Figure IV.4.3 illustrates these examples.

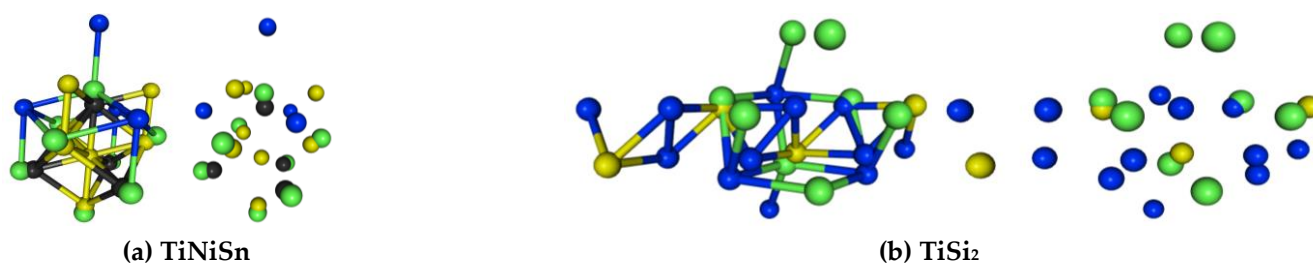


Figure IV.4.3 Illustrations of candidates superposed to Ca_2Si 1009733.

Tables are merged for the rest of the compounds. The next compound that we compare to the others is $\text{C}_{24}\text{N}_{24}$ [491]. Since it is inherently very different, we can see in Table IV.4.12 the few results that may be pursued for finding other useful similarities [492]. Unfortunately parameters from different sources are calculated in different ways. This is why databases are useful, they keep a standard.

Predicted formation energy ^a eV/atom	Aligned compound and index	TM-score	Selected atoms from aligned structure	Eigenvalues for atoms of aligned structure	Selected atoms from $\text{C}_{24}\text{N}_{24}$	Eigenvalues for atoms of $\text{C}_{24}\text{N}_{24}$
-7.99 -> -3.9	$\text{C}_{24}\text{N}_{24}$					
	SnS_2			-54.3838		-408.7987
-0.473	9984 90	0.8836	SnSSSn	-136.9370 -289.0952	CCCC	-45.0393 -26.5720
	SnSb			-40.1638		-356.7474
0.117	1218916 818	0.9001	SbSnSnSn	-187.5463 -213.1920	CNNN	-15.4485 -68.6203
	TiS_2			-2.6029		-17.3752
-1.603	1062030 563	0.9169	TiSTiS	-21.9074 -92.7354	CNNN	-76.6393 -23.4884
	VCIO			-64.6006		-19.0713
-2.193	23061 99	0.8562	CIVOV	-225.9899 -441.7851	CNCC	-74.2268 -639.0813

^a Materials Data by Materials Project in references [25–40, 295–490].

Table IV.4.12 Similarities between $\text{C}_{24}\text{N}_{24}$ and other candidates.

Our next subject is LiMn_2O_4 , material 1045561, presented in Table IV.4.13:

Energy above Hull ^a eV/atom	Band gap ^a eV	Predicted formation energy ^a eV/atom	Space group (internal number) ^a [493]	Aligned compound	TM-score	Number of atoms matched	Observations
0.073	0	-1.992	10	LiMn_2O_4 1045561			
0.117	0	0.117	160	SnSb 1218916	0.8542	4	far apart
0.004	0.05	-1.603	12	TiS_2 1062030	0.9105	4	similar group

^a Materials Data by Materials Project in references [25–40, 295–490].

Table IV.4.13 Similarities between LiMn_2O_4 (material 1045561) and other candidates.

It is normal that some candidates just aren't geometrically similar to any others, as can be seen in Tables IV.4.12-13.

The full thesis provides even more examples of results.

V. Final conclusions and outlook

High-Throughput Screening is a result of applying computational algorithms and machine learning techniques. Researchers can quickly identify materials with desirable properties.

This thesis searches for similarities between compounds used in redox equilibria of energy storage systems. The introduction presents a way of thinking and the structure of this work.

The second chapter illustrates three short reviews: energy storage systems, computational modeling, the kind of similarities that geometrically matched compounds may present and what can be realized with such information.

The third chapter illustrates our objective.

Subchapters in chapter IV contain, in part, published articles that relate to this thesis. Practically, it all starts by choosing a topological index that can be used in similarity search between chemical compounds with applications in energy storage systems. Some counting polynomials are computed for one compound of interest and relations are presented between them. In the end only one polynomial is used and that is the characteristic polynomial.

Subchapter IV.2 presents some extensions that the characteristic polynomial can accommodate and computes area and volume for congeners of C₂₀ fullerene. Fullerenes are rarely employed in energy storage systems, and we try to find any possible similarities with other compounds. Another extension was chosen in the end that will give similarity results for compounds with applications in energy storage systems.

At some point, when there is enough data, patterns can be found in similarities by using iterative methods for solving nonlinear equations.

The chapter ends with the last published work at the moment of thesis submission. Making use of the extension possibilities that the characteristic polynomial offers, the polynomial of the antisymmetric Cartesian distance matrix is computed for all candidates with fewer atoms. These numbers are evaluated for similarities and one detailed result is presented.

Data displayed in the first four columns of Tables IV.4.11-46 is used to find other similarities and evaluate geometrical similarities found by our program. More comparable parameters are necessary to further filter similar compounds and give valuable information about their applications in energy storage systems.

Improvements to the program's code are presented (written in MATLAB [494], with notes presented in Appendix G Programming notes, and fully available in Appendix H Final code), and enumerates some results in order to extract conclusions about the applicability of this work. Although the pairs of sums of eigenvalues are similar, not all such pairs have a correspondence between singular eigenvalues. These results are not published at the moment of writing. The search had to stop somewhere and it did at 293 compared candidates. The alignments offered by the program allow simple discrimination after visualizing superposed candidates.

An important improvement of the code is vectorization (revising loop-based, scalar-oriented code to use Matlab matrix and vector operations). This improvement also relieves the issue of pre-allocating array size. Further improvement should include a way to limit the minimum number of matched atoms, a way to split large compounds so that memory does not present a problem, and a way to use data from other databases in order to pre-eliminate compounds with no other similarity to the one of reference. This last wish also requires databases to keep growing similar to protein databases.

Other scoring functions, possibly derived by extending polynomials should also be tested. An interesting solution is the immanantal polynomial, which unifies other polynomials. Other unifying polynomials have been developed and can be tried.

Objectives are attained, and further publications will improve on them. A script is developed that obtains geometrical similarities with scores that can be used to organise databases of compounds with applications in energy storage systems.

Visualizing similarities is aided by exporting aligned candidates and providing a way of finding the candidate one wishes to compare. Examples are given.

Negative results are exemplified, with the space group number providing easy elimination of coincidences. After visualising, it is sometimes clear that some similarities exist only in a straight line or a plane. These should also be considered coincidences.

More parameters need to be added to databases so that they can be compared in a consistent fashion. It is shown that similar parameters exist between found geometrical similarities.

Table IV.4.47 presents statistics of found similarities. Parameters could be used to reduce the number of superposed candidates that need to be visualised. In the context that one would pursue a similar search of compounds that could replace another; examples of results reveal, for the first 25 candidates, that on average, 1.2 % of rotations give a score greater than 0.85; 18.4 % of candidates' present geometrical similarities to each other and 15.3 % of those also present other similar parameters. Further adding data up until 38 candidates, these numbers change to 1.3 %, 19.8 % and 13.2 %. The growing number of found geometrical similarities reveals that chemical applications can only be found for the obtained data by using more parameters to filter negative results. The descending number of candidates that present other similar parameters supports this reasoning.

In the end it is desirable that few compounds are found similar to each other in order to reduce the number of experiments that need to be carried out in order to confirm or negate the usefulness of found results.

Unfortunately parameters from different sources are calculated in different ways. This is another reason for databases to keep growing. They keep a standard measurement technique. This also means that more compounds are desirable to be analysed by the current methodology in order to create a database of geometrical similarities.

Deeper understanding of the electron transfer processes, charge storage mechanisms, and overall reaction kinetics, can be achieved by studying the geometries of compounds involved in these systems: how electrons are transferred between different oxidation states and how the geometrical arrangement of atoms influences the ease and efficiency of electron transfer; identify possible structural features that enable efficient charge storage, such as the presence of redox-active sites, the accessibility of active sites for ion diffusion, or the ability to accommodate changes in oxidation states without significant structural rearrangements; presence of stable coordination geometries or the ability to withstand structural changes during repeated cycling.

References

1. Mohamed, N.; Allam, N.K. Recent Advances in the Design of Cathode Materials for Li-Ion Batteries. *RSC Adv.* **2020**, *10*, 21662–21685, doi:10.1039/D0RA03314F.
2. Osterloh, W.R.; Conradie, J.; Alemayehu, A.B.; Ghosh, A.; Kadish, K.M. The Question of the Redox Site in Metal–Metal Multiple-Bonded Metalloporphyrin Dimers. *ACS Org. Inorg. Au* **2023**, *3*, 35–40, doi:10.1021/acsorginorgau.2c00030.
3. Parvathy A.S. Advanced Anode and Cathode Materials for Li-Ion Batteries: Application to Printing Methodology. PhD Thesis, Karlsruhe Institut für Technologie, **2021**, doi:10.5445/IR/1000137243.
4. Mutter, D.; Urban, D.F.; Elsässer, C. Computational Analysis of Composition-Structure-Property Relationships in NZP-Type Materials for Li-Ion Batteries. *J. Appl. Phys.* **2019**, *125*, 215115, doi:10.1063/1.5091969.
5. Behbahan, A.S.; Alizadeh, A.; Mahmoudi, M.; Shamsborhan, M.; Al-Musawi, T.J.; Pasha, P. A New Adomian Decomposition Technique for a Thermal Analysis Forced Non-Newtonian Magnetic Reiner-Rivlin Viscoelastic Fluid Flow. *Alex. Eng. J.* **2023**, *80*, 48–57, doi:10.1016/j.aej.2023.08.036.
6. Fika, P. Approximation of the Tikhonov Regularization Parameter through Aitken's Extrapolation. *Appl. Numer. Math.* **2023**, *190*, 270–282, doi:10.1016/j.apnum.2023.04.008.
7. Gutierrez, C.; Gutierrez, F.; Rivara, M.-C. Complexity of the Bisection Method. *Theor. Comput. Sci.* **2007**, *382*, 131–138, doi:10.1016/j.tcs.2007.03.004.
8. Sharma, H.; Kansal, M. A Modified Chebyshev–Halley-type Iterative Family with Memory for Solving Nonlinear Equations and Its Stability Analysis. *Math. Methods in App. Sci.* **2023**, *46*, 12549–12569, doi:10.1002/mma.9197.

9. Petković, I.; Herceg, Đ. Computers in Mathematical Research: The Study of Three-Point Root-Finding Methods. *Numer. Algor.* **2020**, *84*, 1179–1198, doi:10.1007/s11075-019-00796-6.
10. Lu, Y.; Tang, Y. Solving Fractional Differential Equations Using Collocation Method Based Onhybrid of Block-Pulse Functions and Taylor Polynomials. *Turk. J. Math.* **2021**, *45*, 1065–1078, doi:10.3906/mat-2006-2.
11. Assari, P.; Dehghan, M. A Meshless Local Galerkin Method for Solving Volterra Integral Equations Deduced from Nonlinear Fractional Differential Equations Using the Moving Least Squares Technique. *Appl. Numer. Math.* **2019**, *143*, 276–299, doi:10.1016/j.apnum.2019.04.014.
12. Farhood, A.K.; Mohammed, O.H. Homotopy Perturbation Method for Solving Time-Fractional Nonlinear Variable-Order Delay Partial Differential Equations. *Partial Differential Equations in Appl. Math.* **2023**, *7*, 100513, doi:10.1016/j.padiff.2023.100513.
13. Argyros, I.K.; Sharma, D.; Argyros, C.I.; Parhi, S.K.; Sunanda, S.K.; Argyros, M.I. Extended Three Step Sixth Order Jarratt-like Methods under Generalized Conditions for Nonlinear Equations. *Arab. J. Math.* **2022**, *11*, 443–457, doi:10.1007/s40065-022-00379-9.
14. Temple, B.; Young, R. Inversion of a Non-Uniform Difference Operator and a Strategy for Nash–Moser. *MAA* **2022**, *29*, 265–294, doi:10.4310/MAA.2022.v29.n3.a3.
15. Pho, K.-H. Improvements of the Newton–Raphson Method. *J. Comput. Appl. Math.* **2022**, *408*, 114106, doi:10.1016/j.cam.2022.114106.
16. Argyros, I.K.; George, S. Local Convergence of Osada’s Method for Finding Zeros with Multiplicity. In *Understanding Banach Spaces*; Sánchez, D.G., Ed.; Nova Science Publishers: Hauppauge, NY, USA, **2019**; 147–151.
17. Christian Beleña Postigo Ostrowski’s Method for Solving Nonlinear Equations and Systems. *JMEA* **2023**, *13*, doi:10.17265/2159-5275/2023.01.001.
18. Ivanov, S.I. General Local Convergence Theorems about the Picard Iteration in Arbitrary Normed Fields with Applications to Super–Halley Method for Multiple Polynomial Zeros. *Mathematics* **2020**, *8*, 1599, doi:10.3390/math8091599.
19. Coclite, G.M.; Fanizzi, A.; Lopez, L.; Maddalena, F.; Pellegrino, S.F. Numerical Methods for the Nonlocal Wave Equation of the Peridynamics. *Appl. Numer. Math.* **2020**, *155*, 119–139, doi:10.1016/j.apnum.2018.11.007.
20. Darvishi, M.T.; Barati, A. A Fourth-Order Method from Quadrature Formulae to Solve Systems of Nonlinear Equations. *Appl. Math. Comput.* **2007**, *188*, 257–261, doi:10.1016/j.amc.2006.09.115.
21. Nisha, S.; Parida, P.K. Super-Halley Method under Majorant Conditions in Banach Spaces. *Cubo* **2020**, *22*, 55–70, doi:10.4067/S0719-06462020000100055.
22. Putri, R.Y.; Wartono, W. Modifikasi Metode Schroder Tanpa Turunan Kedua Dengan Orde Konvergensi Empat. *AKS* **2020**, *11*, 240–251, doi:10.26877/aks.v11i2.6060.
23. Sharma, J.R.; Kumar, D.; Argyros, I.K. An Efficient Class of Traub–Steffensen-Like Seventh Order Multiple-Root Solvers with Applications. *Symmetry* **2019**, *11*, 518, doi:10.3390/sym11040518.
24. Jamaludin, N.A.A.; Nik Long, N.M.A.; Salimi, M.; Sharifi, S. Review of Some Iterative Methods for Solving Nonlinear Equations with Multiple Zeros. *Afr. Mat.* **2019**, *30*, 355–369, doi:10.1007/s13370-018-00650-3.
25. Jain, A.; Ong, S.P.; Hautier, G.; Chen, W.; Richards, W.D.; Dacek, S.; Cholia, S.; Gunter, D.; Skinner, D.; Ceder, G.; et al. Commentary: The Materials Project: A Materials Genome Approach to Accelerating Materials Innovation. *APL Materials* **2013**, *1*, 011002, doi:10.1063/1.4812323.
26. De Jong, M.; Chen, W.; Geerlings, H.; Asta, M.; Persson, K.A. A Database to Enable Discovery and Design of Piezoelectric Materials. *Sci. Data* **2015**, *2*, 150053, doi:10.1038/sdata.2015.53.

27. Wang, A.; Kingsbury, R.; McDermott, M.; Horton, M.; Jain, A.; Ong, S.P.; Dwaraknath, S.; Persson, K. A Framework for Quantifying Uncertainty in DFT Energy Corrections. *Sci. Rep.* **2021**, *11*, 15496, doi:10.1038/s41598-021-94550-5.
28. Munro, J.M.; Latimer, K.; Horton, M.K.; Dwaraknath, S.; Persson, K.A. An Improved Symmetry-Based Approach to Reciprocal Space Path Selection in Band Structure Calculations. *npj Comput. Mater.* **2020**, *6*, 112, doi:10.1038/s41524-020-00383-7.
29. De Jong, M.; Chen, W.; Angsten, T.; Jain, A.; Notestine, R.; Gamst, A.; Sluiter, M.; Krishna Ande, C.; Van Der Zwaag, S.; Plata, J.J.; et al. Charting the Complete Elastic Properties of Inorganic Crystalline Compounds. *Sci. Data* **2015**, *2*, 150009, doi:10.1038/sdata.2015.9.
30. Ding, H.; Dwaraknath, S.S.; Garten, L.; Ndione, P.; Ginley, D.; Persson, K.A. Computational Approach for Epitaxial Polymorph Stabilization through Substrate Selection. *ACS Appl. Mater. Interfaces* **2016**, *8*, 13086–13093, doi:10.1021/acsami.6b01630.
31. Patel, A.M.; Nørskov, J.K.; Persson, K.A.; Montoya, J.H. Efficient Pourbaix Diagrams of Many-Element Compounds. *Phys. Chem. Chem. Phys.* **2019**, *21*, 25323–25327, doi:10.1039/C9CP04799A.
32. Singh, A.K.; Zhou, L.; Shinde, A.; Suram, S.K.; Montoya, J.H.; Winston, D.; Gregoire, J.M.; Persson, K.A. Electrochemical Stability of Metastable Materials. *Chem. Mater.* **2017**, *29*, 10159–10167, doi:10.1021/acs.chemmater.7b03980.
33. Latimer, K.; Dwaraknath, S.; Mathew, K.; Winston, D.; Persson, K.A. Evaluation of Thermodynamic Equations of State across Chemistry and Structure in the Materials Project. *npj Comput. Mater.* **2018**, *4*, 40, doi:10.1038/s41524-018-0091-x.
34. Jain, A.; Hautier, G.; Ong, S.P.; Moore, C.J.; Fischer, C.C.; Persson, K.A.; Ceder, G. Formation Enthalpies by Mixing GGA and GGA + U Calculations. *Phys. Rev. B* **2011**, *84*, 045115, doi:10.1103/PhysRevB.84.045115.
35. Zheng, H.; Li, X.-G.; Tran, R.; Chen, C.; Horton, M.; Winston, D.; Persson, K.A.; Ong, S.P. Grain Boundary Properties of Elemental Metals. *Acta Materialia* **2020**, *186*, 40–49, doi:10.1016/j.actamat.2019.12.030.
36. Horton, M.K.; Montoya, J.H.; Liu, M.; Persson, K.A. High-Throughput Prediction of the Ground-State Collinear Magnetic Order of Inorganic Materials Using Density Functional Theory. *npj Comput. Mater.* **2019**, *5*, 64, doi:10.1038/s41524-019-0199-7.
37. Petousis, I.; Mrdjenovich, D.; Ballouz, E.; Liu, M.; Winston, D.; Chen, W.; Graf, T.; Schladt, T.D.; Persson, K.A.; Prinz, F.B. High-Throughput Screening of Inorganic Compounds for the Discovery of Novel Dielectric and Optical Materials. *Sci. Data* **2017**, *4*, 160134, doi:10.1038/sdata.2016.134.
38. Persson, K.A.; Waldwick, B.; Lazic, P.; Ceder, G. Prediction of Solid-Aqueous Equilibria: Scheme to Combine First-Principles Calculations of Solids with Experimental Aqueous States. *Phys. Rev. B* **2012**, *85*, 235438, doi:10.1103/PhysRevB.85.235438.
39. Tran, R.; Xu, Z.; Radhakrishnan, B.; Winston, D.; Sun, W.; Persson, K.A.; Ong, S.P. Surface Energies of Elemental Crystals. *Sci. Data* **2016**, *3*, 160080, doi:10.1038/sdata.2016.80.
40. Aykol, M.; Dwaraknath, S.S.; Sun, W.; Persson, K.A. Thermodynamic Limit for Synthesis of Metastable Inorganic Materials. *Sci. Adv.* **2018**, *4*, eaaq0148, doi:10.1126/sciadv.aaq0148.
41. Ntie-Kang, F.; Yong, J.N. The Chemistry and Biological Activities of Natural Products from Northern African Plant Families: From Aloaceae to Cupressaceae. *RSC Adv.* **2014**, *4*, 61975–61991, doi:10.1039/C4RA11467A.
42. Mypati, S.; Khazaeli, A.; Barz, D.P.J. A Novel Rechargeable Zinc–Copper Battery without a Separator. *J. Energy Storage* **2021**, *42*, 103109, doi:10.1016/j.est.2021.103109.

43. Jäntschi, L. Potential of Electrical Cells: The Effect of the Experimental Design on the Results. In Proceedings of the 2023 International Conference on Clean Electrical Power (ICCEP); IEEE: Terrasini, Italy, June 27 2023; 622–629.
44. Stoenoiu, C.E.; Jäntschi, L. Simultaneous Determinations for the Internal Resistance of Three Batteries. Three Analytical Methods Involved. In Proceedings of the 2023 10th International Conference on Modern Power Systems (MPS); IEEE: Cluj-Napoca, Romania, June 21 2023; 01–05.
45. Ye, H.; Ng, J. Shielding Effects of Myelin Sheath on Axolemma Depolarization under Transverse Electric Field Stimulation. *PeerJ* **2018**, *6*, e6020, doi:10.7717/peerj.6020.
46. Younesi, R. Batteries: An Important Piece in the Puzzle of Renewable Energies for a Better World. *Front. Energy Res.* **2014**, *2*, doi:10.3389/fenrg.2014.00014.
47. Walker, R. Church of England Clergyman and Physicist. In *The Oxford Dictionary of National Biography*; Matthew, H.C.G., Harrison, B., Simcock, A.V., Eds.; Oxford University Press: Oxford, **2004** ISBN 978-0-19-861412-8.
48. Chambers, W.; Chambers, R. *Chambers's Journal of Popular Literature, Science and Arts*; Fourth series; Cornell University, **1873**; 10.
49. Berg, H. Johann Wilhelm Ritter - The Founder of Scientific Electrochemistry. *Rev. Polarogr.* **2008**, *54*, 99–103, doi:10.5189/revpolarography.54.99.
50. Tinazzi, M. *The Life and the Work of Giuseppe Zamboni at the Light of His Unpublished Letters*; Liceo Scientifico "G. Fracastoro", via Moschini 11, **2013**, Available Online: <http://www.sisfa.org/wp-content/uploads/2013/03/xviiTinazzi.pdf> (Accessed on 10 February 2024).
51. Wisniak, J. William Hyde Wollaston. The platinum group metals and other discoveries. *Educ. Química* **2018**, *17*, 130, doi:10.22201/fq.18708404e.2006.2.66052.
52. Kosky, P.; Balmer, R.; Keat, W.; Wise, G. Electrochemical Engineering. In *Exploring Engineering*; Elsevier, **2021**; 383–403 ISBN 978-0-12-815073-3.
53. Murray, J. *Bird's First Publication of His Modification of the Daniell Cell*; Seventh Meeting of the British Society for the Advancement of Science; London, **1837**; 45.
54. Jindal, S.L. A Useful Electric Cell. *Nature* **1927**, *119*, 639–639, doi:10.1038/119639a0.
55. Sallami, A.; Mzoughi, D.; Mami, A. Robust Diagnosis of a Proton Exchange Membrane Fuel Cell Using Bond Graph Methodology – Physical and Electrical Faults Detection and Isolation. *Adv. Sci. Technol. Res. J.* **2019**, *13*, 194–203, doi:10.12913/22998624/111704.
56. *A Dictionary of Electronics and Electrical Engineering*; Butterfield, A.J., Szymanski, J., Eds.; Oxford University Press, **2018**; Vol. 1; 720 ISBN 978-0-19-872572-5.
57. Bunsen, R. Ueber Die Anwendung Der Kohle Zu Volta'schen Batterien. *Annalen der Physik* **1841**, *130*, 417–430, doi:10.1002/andp.18411301109.
58. Kuratani, K.; Fukami, K.; Tsuchiya, H.; Usui, H.; Chiku, M.; Yamazaki, S. Electrochemical Polarization Part 1: Fundamentals and Corrosion. *Electrochemistry* **2022**, *90*, 102003–102003, doi:10.5796/electrochemistry.22-66085.
59. Padmaraj, D.; Miller, J.H.; Wosik, J.; Zagozdzon-Wosik, W. Reduction of Electrode Polarization Capacitance in Low-Frequency Impedance Spectroscopy by Using Mesh Electrodes. *Biosens. Bioelectron.* **2011**, *29*, 13–17, doi:10.1016/j.bios.2011.06.050.
60. Huang, Z.; Mu, A. Research and Analysis of Performance Improvement of Vanadium Redox Flow Battery in Microgrid: A Technology Review. *Intl. J. Energy Res.* **2021**, *45*, 14170–14193, doi:10.1002/er.6716.

61. Qi, M.-Y.; Xu, Y.-S.; Guo, S.-J.; Zhang, S.-D.; Li, J.-Y.; Sun, Y.-G.; Jiang, K.-C.; Cao, A.-M.; Wan, L.-J. The Functions and Applications of Fluorinated Interface Engineering in Li-Based Secondary Batteries. *Small Sci.* **2021**, *1*, 2100066, doi:10.1002/smsc.202100066.
62. Pali-Casanova, R.; Yam-Cervantes, M.; Zavala-Loría, J.; Loría-Bastarrachea, M.; Aguilar-Vega, M.; Dzul-López, L.; Sámano-Celorio, M.; Crespo-Álvarez, J.; García-Villena, E.; Agudo-Toyos, P.; et al. Effect of Sulfonic Groups Concentration on IEC Properties in New Fluorinated Copolyamides. *Polymers* **2019**, *11*, 1169, doi:10.3390/polym11071169.
63. King, W.J. *The Development of Electrical Technology in the 19th Century: The Electrochemical Cell and the Electromagnet*; Bulletin; Smithsonian Institute, **1962**.
64. Newman, J.S.; Thomas-Alyea, K.E. *Electrochemical Systems*; 3rd ed.; J. Wiley: Hoboken, N.J, **2004**; 647 ISBN 978-0-471-47756-3.
65. Alfred Dun Patent US312339A Galvanic Element **1885**.
66. Carl Gassner Patent US373064A Galvanic Battery **1887**.
67. Efe, Ş.; Güngör, Z.A. Geçmişten Günümüze Batarya Teknolojisi. *EJOSAT* **2022**, doi:10.31590/ejosat.1048673.
68. Pickard, W.F. Massive Electricity Storage for a Developed Economy of Ten Billion People. *IEEE Access* **2015**, *3*, 1392–1407, doi:10.1109/ACCESS.2015.2469255.
69. Edison, T. Catalogue of Edison-Lalande Batteries, Edison Motors and Fan Outfits, Edison Projecting Kinetoscopes, Edison X-Ray Apparatus, Edison Cautery. *Edison Manufacturing Company* **1910**, *28*, Available Online: archive.org/details/catalogueofediso00edis (Accessed on 10 February 2024).
70. Mauger, A.; Julien, C.M. Critical Review on Lithium-Ion Batteries: Are They Safe? Sustainable? *Ionics* **2017**, *23*, 1933–1947, doi:10.1007/s11581-017-2177-8.
71. Edelmann, F. The Life and Legacy of Thomas Midgley Jr. *PPRST* **2016**, *150*, 45–49, doi:10.26749/rstpp.150.1.45.
72. George W.H. Patent US1899615A Air-Depolarized Primary Battery **1925**.
73. Marsal, P.A.; Karl, K.; Urry, L.F. Patent US2960558A Dry Cell **1957**.
74. Krishna Sapru; Benjamin Reichman; Arie Reger; Stanford R. Ovshinsky Patent US4623597A Rechargeable Battery and Electrode Used Therein **1985**.
75. Wang, Y.; Li, T.; Li, Y.; Yang, R.; Zhang, G. 2D-Materials-Based Wearable Biosensor Systems. *Biosensors* **2022**, *12*, 936, doi:10.3390/bios12110936.
76. Zheng, X.; Jiang, W.; Yin, L.; Fu, Y. Optimal Energy Allocation Algorithm of Li-Battery/Super Capacitor Hybrid Energy Storage System Based on Dynamic Programming Algorithm. *E3S Web Conf.* **2021**, *231*, 01001, doi:10.1051/e3sconf/202123101001.
77. Moss, J.B. Computational and Experimental Studies on Energy Storage Materials and Electrocatalysts. PhD Thesis, Utah State University, **2019**, doi:10.26076/ER73-DY50.
78. Vanderbruggen, A. Lithium Ion Batteries Recycling with Froth Flotation - A Study on Characterization and Liberation Strategies. PhD Thesis, Aalto University, **2022**.
79. Marvin Messing Advanced Characterization of Battery Cell Dynamics. PhD Thesis, McMaster University, **2021**.
80. Marie-Therese von Srbik Advanced Lithium-Ion Battery Modelling for Automotive Applications. PhD Thesis, Imperial College London, **2015**.
81. Claudio Brivio Battery Energy Storage Systems: Modelling, Applications and Design Criteria. PhD Thesis, Politecnico Di Milano, **2017**.
82. Christian Achim Hellwig Modeling, Simulation and Experimental Investigation of the Thermal and Electrochemical Behavior of a LiFePO₄-Based Lithium-Ion Battery. PhD Thesis, Universität Stuttgart, **2013**.

83. Marc Dylan Berliner Simulating, Controlling, and Understanding Lithium-Ion Battery Models. PhD Thesis, Massachusetts Institute of Technology, **2023**.
84. Rutooj D. Deshpande Understanding and Improving Lithium Ion Batteries through Mathematical Modeling and Experiments. PhD Thesis, University of Kentucky, **2011**.
85. Trevisanello, E.; Ruess, R.; Conforto, G.; Richter, F.H.; Janek, J. Polycrystalline and Single Crystalline NCM Cathode Materials—Quantifying Particle Cracking, Active Surface Area, and Lithium Diffusion. *Adv. Energy Mater.* **2021**, *11*, 2003400, doi:10.1002/aenm.202003400.
86. Gheyztanzadeh, M.; Baghban, A.; Habibzadeh, S.; Mohaddespour, A.; Abida, O. Insights into the Estimation of Capacitance for Carbon-Based Supercapacitors. *RSC Adv.* **2021**, *11*, 5479–5486, doi:10.1039/D0RA09837J.
87. Liu, Y.; Ma, C.; Wang, K.; Chen, J. Recent Advances in Porous Carbons for Electrochemical Energy Storage. *New Carbon Mate.* **2023**, *38*, 1–15, doi:10.1016/S1872-5805(23)60710-3.
88. Kartsonakis, I.A. Special Issue on “Phase Change Materials: Design and Applications.” *Appl. Sci.* **2022**, *12*, 7770, doi:10.3390/app12157770.
89. Diudea, M.V. Counting Polynomials in Tori $T(4,4)S[c,n]$. *Acta Chim. Slov.* **2010**, *57*, 551–558.
90. Eliasi, M.; Taeri, B. Extension of the Wiener Index and Wiener Polynomial. *Appl. Math. Lett.* **2008**, *21*, 916–921, doi:10.1016/j.aml.2007.10.001.
91. Parveen, S.; Awan, N.U.H.; Farooq, F.B.; Hussain, S. Topological Descriptors and QSPR Models of Drugs Used in Blood Cancer. *Punjab Univ. J. Math.* **2023**, *55*, 27–43, doi:10.52280/pujm.2023.550103.
92. Alviso, D.; Aguerre, H.; Nigro, N.; Artana, G. Prediction of the Physico-Chemical Properties of Vegetable Oils Using Optimal Non-Linear Polynomials. *Fuel* **2023**, *350*, 128868, doi:10.1016/j.fuel.2023.128868.
93. Calingaert, G.; Hladky, J.W. A Method of Comparison and Critical Analysis of the Physical Properties of Homologs and Isomers. The Molecular Volume of Alkanes *. *J. Am. Chem. Soc.* **1936**, *58*, 153–157, doi:10.1021/ja01292a044.
94. Kurtz, S.S.; Lipkin, M.R. Molecular Volume of Saturated Hydrocarbons. *Ind. Eng. Chem.* **1941**, *33*, 779–786, doi:10.1021/ie50378a021.
95. Wiener, H. Structural Determination of Paraffin Boiling Points. *J. Am. Chem. Soc.* **1947**, *69*, 17–20, doi:10.1021/ja01193a005.
96. Liu, J.-B.; Javed, S.; Javid, M.; Shabbir, K. Computing First General Zagreb Index of Operations on Graphs. *IEEE Access* **2019**, *7*, 47494–47502, doi:10.1109/ACCESS.2019.2909822.
97. *Chemical Graph Theory: Introduction and Fundamentals*; Bonchev, D., Rouvray, D.H., Eds.; Mathematical chemistry; Abacus Press: New York, **1991**; 300 ISBN 978-0-85626-454-2.
98. Dalton, J.; Scattergood, T.; Thorpe, T.E. *A New System of Chemical Philosophy*; Printed by S. Russell for R. Bickerstaff, London: Manchester, **1808**; 600.
99. Wollaston, W.H. On Super-Acid and Sub-Acid Salts. *Philos. Trans. R. Soc. Lond., B, Biol. Sci.* **1808**, *98*, 96–102.
100. Kopp, H. Ueber den Zusammenhang zwischen der chemischen Constitution und einigen physikalischen Eigenschaften bei flüssigen Verbindungen. *Ann. Chem. Pharm.* **1844**, *50*, 71–144, doi:10.1002/jlac.18440500105.
101. Cayley, E. LVII. On the Mathematical Theory of Isomers. *Lond. Edinb. Dublin Philos. Mag. J. Sci.* **1874**, *47*, 444–447, doi:10.1080/14786447408641058.
102. Cayley, E. Ueber Die Analytischen Figuren, Welche in Der Mathematik Bäume Genannt Werden Und Ihre Anwendung Auf Die Theorie Chemischer Verbindungen. *Ber. Dtsch. Chem. Ges.* **1875**, *8*, 1056–1059, doi:10.1002/cber.18750080252.

103. Sylvester, J.J. On an Application of the New Atomic Theory to the Graphical Representation of the Invariants and Covariants of Binary Quantics, with Three Appendices. *Am. J. Math.* **1878**, *1*, 64, doi:10.2307/2369436.
104. Pólya, G. Kombinatorische Anzahlbestimmungen Für Gruppen, Graphen Und Chemische Verbindungen. *Acta Math.* **1937**, *68*, 145–254, doi:10.1007/BF02546665.
105. Platt, J.R. Prediction of Isomeric Differences in Paraffin Properties. *J. Phys. Chem.* **1952**, *56*, 328–336, doi:10.1021/j150495a009.
106. Platt, J.R. Influence of Neighbor Bonds on Additive Bond Properties in Paraffins. *J. Chem. Phys.* **1947**, *15*, 419–420, doi:10.1063/1.1746554.
107. Gordon, M.; Scantlebury, G.R. Non-Random Polycondensation : Statistical Theory of the Substitution Effect. *Trans. Faraday Soc.* **1964**, *60*, 604, doi:10.1039/tf9646000604.
108. Hosoya, H. Topological Index. A Newly Proposed Quantity Characterizing the Topological Nature of Structural Isomers of Saturated Hydrocarbons. *BCSJ* **1971**, *44*, 2332–2339, doi:10.1246/bcsj.44.2332.
109. Gutman, I.; Rušćić, B.; Trinajstić, N.; Wilcox, C.F. Graph Theory and Molecular Orbitals. XII. Acyclic Polyenes. *J. Chem. Phys.* **1975**, *62*, 3399–3405, doi:10.1063/1.430994.
110. Balaban, A.T. Chemical Graphs: XXXIV. Five New Topological Indices for the Branching of Tree-like Graphs [1]. *Theoret. Chim. Acta* **1979**, *53*, 355–375, doi:10.1007/BF00555695.
111. Bonchev, D.; Balaban, A.T.; Mekenyan, O. Generalization of the Graph Center Concept, and Derived Topological Centric Indexes. *J. Chem. Inf. Comput. Sci.* **1980**, *20*, 106–113, doi:10.1021/ci60022a011.
112. Bonchev, D.; Balaban, A.T.; Randić, M. The Graph Center Concept for Polycyclic Graphs. *Int. J. Quantum Chem.* **1981**, *19*, 61–82, doi:10.1002/qua.560190107.
113. Bonchev, D.; Mekenyan, O.; Balaban, A.T. Iterative Procedure for the Generalized Graph Center in Polycyclic Graphs. *J. Chem. Inf. Comput. Sci.* **1989**, *29*, 91–97, doi:10.1021/ci00062a007.
114. Schultz, H.P. Topological Organic Chemistry. 1. Graph Theory and Topological Indices of Alkanes. *J. Chem. Inf. Comput. Sci.* **1989**, *29*, 227–228, doi:10.1021/ci00063a012.
115. Schultz, H.P.; Schultz, E.B.; Schultz, T.P. Topological Organic Chemistry. 2. Graph Theory, Matrix Determinants and Eigenvalues, and Topological Indexes of Alkanes. *J. Chem. Inf. Comput. Sci.* **1990**, *30*, 27–29, doi:10.1021/ci00065a007.
116. Randić, M. Characterization of Molecular Branching. *J. Am. Chem. Soc.* **1975**, *97*, 6609–6615, doi:10.1021/ja00856a001.
117. Kier, L.B.; Hall, L.H. *Molecular Connectivity in Structure-Activity Analysis*; Chemometrics series; Research Studies Press; Wiley: Letchworth, Hertfordshire, England; New York, **1986**; 280 ISBN 978-0-471-90983-5.
118. Kier, L.B.; Hall, L.H. *Molecular Connectivity in Chemistry and Drug Research*; Medicinal chemistry; Academic Press: New York, **1976**; 257 ISBN 978-0-12-406560-4.
119. Kier, L.B.; Hall, L.H.; Murray, W.J.; Randić, M. Molecular Connectivity I: Relationship to Nonspecific Local Anesthesia. *J. Pharm. Sci.* **1975**, *64*, 1971–1974, doi:10.1002/jps.2600641214.
120. Kier, L.B.; Murray, W.J.; Randić, M.; Hall, L.H. Molecular Connectivity V: Connectivity Series Concept Applied to Density. *J. Pharm. Sci.* **1976**, *65*, 1226–1230, doi:10.1002/jps.2600650824.
121. Bonchev, D.; Trinajstić, N. Information Theory, Distance Matrix, and Molecular Branching. *J. Chem. Phys.* **1977**, *67*, 4517–4533, doi:10.1063/1.434593.
122. Merrifield, R.E.; Simmons, H.E. The Structures of Molecular Topological Spaces. *Theoret. Chim. Acta* **1980**, *55*, 55–75, doi:10.1007/BF00551410.
123. Merrifield, R.E.; Simmons, H.E. Enumeration of Structure-Sensitive Graphical Subsets: Calculations. *Proc. Natl. Acad. Sci. U.S.A.* **1981**, *78*, 1329–1332.

124. Merrifield, R.E.; Simmons, H.E. Enumeration of Structure-Sensitive Graphical Subsets: Theory. *Proc. Natl. Acad. Sci. U.S.A.* **1981**, *78*, 692–695.
125. Bonchev, D.; Mekenyan, O.V.; Trinajstić, N. Isomer Discrimination by Topological Information Approach. *J. Comput. Chem.* **1981**, *2*, 127–148, doi:10.1002/jcc.540020202.
126. Balaban, A.T. Highly Discriminating Distance-Based Topological Index. *Chem. Phys. Lett.* **1982**, *89*, 399–404, doi:10.1016/0009-2614(82)80009-2.
127. Basak, S.C.; Magnuson, V.R. Molecular Topology and Narcosis. A Quantitative Structure-Activity Relationship (QSAR) Study of Alcohols Using Complementary Information Content (CIC). *Arzneimittelforschung* **1983**, *33*, 501–503.
128. Bertz, S.H. Branching in Graphs and Molecules. *Discrete Appl. Math.* **1988**, *19*, 65–83, doi:10.1016/0166-218X(88)90006-6.
129. Kier, L.B.; Hall, L.H. An Electrotopological-State Index for Atoms in Molecules. *Pharm. Res.* **1990**, *7*, 801–807, doi:10.1023/a:1015952613760.
130. Hall, L.H.; Kier, L.B. Electrotopological State Indices for Atom Types: A Novel Combination of Electronic, Topological, and Valence State Information. *J. Chem. Inf. Comput. Sci.* **1995**, *35*, 1039–1045, doi:10.1021/ci00028a014.
131. Lovász, L.; Pelikán, J. On the Eigenvalues of Trees. *Period. Math. Hung.* **1973**, *3*, 175–182, doi:10.1007/BF02018473.
132. Filip, P.A.; Balaban, T.-S.; Balaban, A.T. A New Approach for Devising Local Graph Invariants: Derived Topological Indices with Low Degeneracy and Good Correlation Ability. *J. Math. Chem.* **1987**, *1*, 61–83, doi:10.1007/BF01205338.
133. Balaban, A.T.; Ivanciuc, O. Historical Development of Topological Indices. In *Topological Indices and Related Descriptors in QSAR and QSPAR*; Devillers, J., Balaban, A.T., Eds.; CRC Press, **2000**; 31–68 ISBN 978-0-429-18059-0.
134. Gutman, I. Degree-Based Topological Indices. *Croat. Chem. Acta* **2013**, *86*, 351–361, doi:10.5562/cca2294.
135. Ghorbani, M.; Hosseinzadeh, M.A. The Third Version Of Zagreb Index. *Discrete Math. Algorithm. Appl.* **2013**, *05*, 1350039, doi:10.1142/S1793830913500390.
136. Gao, W.; Farahani, M.R.; Jamil, M.K. The Eccentricity Version of Atom-Bond Connectivity Index of Linear Polycene Parallelogram Benzenoid $ABC_5(P(n,n))$. *Acta Chim. Slov.* **2016**, *63*, 376–379, doi:10.17344/acsi.2016.2378.
137. Hosamani, S.M. Computing Sanskruti Index of Certain Nanostructures. *J. Appl. Math. Comput.* **2017**, *54*, 425–433, doi:10.1007/s12190-016-1016-9.
138. Gao, W.; Wang, Y.; Wang, W.; Shi, L. The First Multiplication Atom-Bond Connectivity Index of Molecular Structures in Drugs. *Saudi Pharm. J.* **2017**, *25*, 548–555, doi:10.1016/j.jsps.2017.04.021.
139. Kulli, V.R. Product Connectivity Leap Index and ABC Leap Index of Helm Graphs. *APAM* **2018**, *18*, 189–192, doi:10.22457/apam.v18n2a8.
140. Mondal, S.; De, N.; Pal, A. On Neighborhood Zagreb Index of Product Graphs. *J. Mol. Struct.* **2021**, *1223*, 129210, doi:10.1016/j.molstruc.2020.129210.
141. Gao, W.; Wang, W. Second Atom-Bond Connectivity Index of Special Chemical Molecular Structures. *J. Chem.* **2014**, *2014*, 1–8, doi:10.1155/2014/906254.
142. Ali, P.; Kirmani, S.A.K.; Al Rugaie, O.; Azam, F. Degree-Based Topological Indices and Polynomials of Hyaluronic Acid-Curcumin Conjugates. *Saudi Pharm. J.* **2020**, *28*, 1093–1100, doi:10.1016/j.jsps.2020.07.010.
143. Mondal, S.; De, N.; Pal, A. Topological Indices of Some Chemical Structures Applied for the Treatment of COVID-19 Patients. *Polycycl. Aromat. Compd.* **2022**, *42*, 1220–1234, doi:10.1080/10406638.2020.1770306.

144. Arockiaraj, M.; Clement, J.; Balasubramanian, K. Analytical Expressions for Topological Properties of Polycyclic Benzenoid Networks. *J. Chemom.* **2016**, *30*, 682–697, doi:10.1002/cem.2851.
145. Ghosh, T.; Mondal, S.; Mondal, S.; Mandal, B. Distance Numbers and Wiener Indices of IPR Fullerenes with Formula $C_{10(n-2)}$ ($n \geq 8$) in Analytical Forms. *Chem. Phys. Lett.* **2018**, *701*, 72–80, doi:10.1016/j.cplett.2018.04.039.
146. Arockiaraj, M.; Clement, J.; Paul, D.; Balasubramanian, K. Quantitative Structural Descriptors of Sodalite Materials. *J. Mol. Struct.* **2021**, *1223*, 128766, doi:10.1016/j.molstruc.2020.128766.
147. Arockiaraj, M.; Clement, J.; Paul, D.; Balasubramanian, K. Relativistic Distance-Based Topological Descriptors of Linde Type A Zeolites and Their Doped Structures with Very Heavy Elements. *Mol. Phys.* **2021**, *119*, e1798529, doi:10.1080/00268976.2020.1798529.
148. Brito, D.; Marquez, E.; Rosas, F.; Rosas, E. Predicting New Potential Antimalarial Compounds by Using Zagreb Topological Indices. *AIP Adv.* **2022**, *12*, 045017, doi:10.1063/5.0089325.
149. Diudea, M.V.; Gutman, I.; Jäntschi, L. *Molecular Topology*; 2nd ed.; Nova Science, Huntington, NY, USA, **2002**; 337 ISBN 978-1-56072-957-0.
150. Park, J.; Moon, J.; Kim, C.; Kang, J.H.; Lim, E.; Park, J.; Lee, K.J.; Yu, S.-H.; Seo, J.-H.; Lee, J.; et al. Graphene Quantum Dots: Structural Integrity and Oxygen Functional Groups for High Sulfur/Sulfide Utilization in Lithium Sulfur Batteries. *NPG Asia Mater.* **2016**, *8*, e272–e272, doi:10.1038/am.2016.61.
151. Attanayake, N.H.; Liang, Z.; Wang, Y.; Kaur, A.P.; Parkin, S.R.; Mobley, J.K.; Ewoldt, R.H.; Landon, J.; Odom, S.A. Dual Function Organic Active Materials for Nonaqueous Redox Flow Batteries. *Mater. Adv.* **2021**, *2*, 1390–1401, doi:10.1039/D0MA00881H.
152. Gong, Y.; Gu, L. Degrees of Freedom for Energy Storage Material. *Carbon Energy* **2022**, *4*, 633–644, doi:10.1002/cey2.195.
153. Lang, S.; Yu, S.-H.; Feng, X.; Krumov, M.R.; Abruña, H.D. Understanding the Lithium–Sulfur Battery Redox Reactions via Operando Confocal Raman Microscopy. *Nat. Commun.* **2022**, *13*, 4811, doi:10.1038/s41467-022-32139-w.
154. Manzi, J.; Paolone, A.; Palumbo, O.; Corona, D.; Massaro, A.; Cavaliere, R.; Muñoz-García, A.B.; Trequattrini, F.; Pavone, M.; Brutti, S. Monoclinic and Orthorhombic NaMnO_2 for Secondary Batteries: A Comparative Study. *Energies* **2021**, *14*, 1230, doi:10.3390/en14051230.
155. Liang, X.; Li, S.; Yang, G.; Wu, X.; Huang, D.; Ning, Y.; Luo, J.; Fang, Z. High Lithium-Ion Conductivity in All-Solid-State Lithium Batteries by Sb Doping LLZO. *Appl. Phys. A* **2022**, *128*, 4, doi:10.1007/s00339-021-05128-x.
156. Ge, L.; Liu, T.; Zhang, Y.; Liu, H. Characterization and Comparison of Organic Functional Groups Effects on Electrolyte Performance for Vanadium Redox Flow Battery. *Front. Chem. Sci. Eng.* **2023**, *17*, 1221–1230, doi:10.1007/s11705-023-2298-8.
157. Zhang, Z.; Gu, Z.; Zhang, C.; Li, J.; Wang, C. Sodium-Ion Capacitors: Recent Development in Electrode Materials. *Batteries & Supercaps.* **2021**, *4*, 1680–1700, doi:10.1002/batt.202100042.
158. Tuo, K.; Yin, F.; Mi, F.; Sun, C. Elucidating the Diffusion Pathway of Lithium Ions in Superionic Halide Solid Electrolytes $\text{Li}_2\text{+Hf1-In Cl}_6$ for All-Solid-State Lithium-Metal Based Batteries. *J. Energy Chem.* **2023**, *87*, 12–23, doi:10.1016/j.jechem.2023.08.016.
159. Sun, G.; Yang, D.; Zhang, Z.; Wang, Y.; Lu, W.; Feng, M. Oxygen Vacancy-Rich MoO_3 Nanorods as Photocatalysts for Photo-Assisted Li-O_2 Batteries. *J. Adv. Ceram.* **2023**, *12*, 747–759, doi:10.26599/JAC.2023.9220717.
160. Yang, S.; Zhang, S.; Dong, W.; Xia, Y. Purification Mechanism of Microcrystalline Graphite and Lithium Storage Properties of Purified Graphite. *Mater. Res. Express* **2022**, *9*, 025505, doi:10.1088/2053-1591/ac513f.

161. Gazda, M.; Kusz, B.; Płończak, P.; Molin, S.; Jasinski, P. Chemical Interaction between Perovskite $\text{La}_{0.6}\text{Sr}_{0.4}\text{FeO}_3$ and Super-Ionic $\text{Zr}_{0.84}\text{Y}_{0.16}\text{O}_x$. *Acta Phys. Pol. A* **2008**, *114*, 135–141, doi:10.12693/APhysPolA.114.135.
162. Metal-Organic Framework MIL-53(Fe) as a Highly Efficient Reusable Catalyst for the Synthesis of 2-Aryl-1H-Benzimidazole. *Chem. Methodol.* **2019**, *3*, 768–776, doi:10.33945/SAMI/CHEMM.2019.6.8.
163. Chen, J.; Lee, P.S. Electrochemical Supercapacitors: From Mechanism Understanding to Multifunctional Applications. *Adv. Energy Mater.* **2021**, *11*, 2003311, doi:10.1002/aenm.202003311.
164. Tang, Z.; Wang, S.; Liao, J.; Wang, S.; He, X.; Pan, B.; He, H.; Chen, C. Facilitating Lithium-Ion Diffusion in Layered Cathode Materials by Introducing $\text{Li}^+/\text{Ni}^{2+}$ Antisite Defects for High-Rate Li-Ion Batteries. *Research* **2019**, *2019*, 2019/2198906, doi:10.34133/2019/2198906.
165. Kong, F.; Cui, X.; Huang, Y.; Yao, H.; Chen, Y.; Tian, H.; Meng, G.; Chen, C.; Chang, Z.; Shi, J. N-Doped Carbon Electrocatalyst: Marked ORR Activity in Acidic Media without the Contribution from Metal Sites? *Angew. Chem.* **2022**, *134*, e202116290, doi:10.1002/ange.202116290.
166. Goel, N.; Kushwaha, A.; Kumar, M. Two-Dimensional MXenes: Recent Emerging Applications. *RSC Adv.* **2022**, *12*, 25172–25193, doi:10.1039/D2RA04354H.
167. Ding, Y.; Zhang, C.; Zhang, L.; Zhou, Y.; Yu, G. Molecular Engineering of Organic Electroactive Materials for Redox Flow Batteries. *Chem. Soc. Rev.* **2018**, *47*, 69–103, doi:10.1039/C7CS00569E.
168. Yano, M.; Suzuki, S.; Miyayama, M.; Ohgaki, M. Electrochemical Properties of Layer-Structured $\text{H}_x(\text{Ni}_{1/3}\text{Co}_{1/3}\text{Mn}_{1/3})\text{O}_2$ for Electrochemical Capacitors in Alkaline Aqueous Solutions. *J. Asian Ceram. Soc.* **2013**, *1*, 71–76, doi:10.1016/j.jascer.2013.03.006.
169. Mahato, N.; Mohapatra, D.; Cho, M.H.; Ahn, K.S. Semi-Polycrystalline–Polyaniline Empowered Electrochemical Capacitor. *Energies* **2022**, *15*, 2001, doi:10.3390/en15062001.
170. Kim, J.; Chae, O.B.; Lucht, B.L. Perspective—Structure and Stability of the Solid Electrolyte Interphase on Silicon Anodes of Lithium-Ion Batteries. *J. Electrochem. Soc.* **2021**, *168*, 030521, doi:10.1149/1945-7111/abe984.
171. Zhen, C.; Wu, T.; Chen, R.; Wang, L.; Liu, G.; Cheng, H.-M. Strategies for Modifying TiO_2 Based Electron Transport Layers to Boost Perovskite Solar Cells. *ACS Sustainable Chem. Eng.* **2019**, *7*, 4586–4618, doi:10.1021/acssuschemeng.8b06580.
172. Joița, D.-M.; Tomescu, M.A.; Jäntschi, L. Counting Polynomials in Chemistry: Past, Present, and Perspectives. *Symmetry* **2023**, *15*, 1815, doi:10.3390/sym15101815.
173. Hosoya, H. On Some Counting Polynomials in Chemistry. *Discrete Appl. Math.* **1988**, *19*, 239–257, doi:10.1016/0166-218X(88)90017-0.
174. Diudea, M.V. Omega Polynomial in Twisted/Chiral Polyhex Tori. *J. Math. Chem.* **2009**, *45*, 309–315, doi:10.1007/s10910-008-9407-2.
175. Müller, J. On the Multiplicity-Free Actions of the Sporadic Simple Groups. *J. Algebra* **2008**, *320*, 910–926, doi:10.1016/j.jalgebra.2008.01.040.
176. Fujita, S. Symmetry-Itemized Enumeration of Cubane Derivatives as Three-Dimensional Entities by the Fixed-Point Matrix Method of the USCI Approach. *BCSJ* **2011**, *84*, 1192–1207, doi:10.1246/bcsj.20110195.
177. Jäntschi, L.; Bolboacă, S.D. Counting Polynomials. In *New Frontiers in Nanochemistry*; Putz, M.V., Ed.; Apple Academic Press, **2020**; 141–148 ISBN 978-0-429-02294-4.
178. Bolboacă, S.-D.; Jäntschi, L. How Good Can the Characteristic Polynomial Be for Correlations? *Int. J. Mol. Sci.* **2007**, *8*, 335–345, doi:10.3390/i8040335.
179. Jäntschi, L.; Bălan, M.C.; Bolboacă, S.-D. Counting Polynomials on Regular Iterative Structures. *Appl. Med. Inform.* **2009**, *24*, 67–95.

180. Gutman, I. Graphs and Graph Polynomials of Interest in Chemistry. In *Graph-Theoretic Concepts in Computer Science*; Tinhofer, G., Schmidt, G., Eds.; Springer: Berlin, Heidelberg, **1987**; Vol. 246, 177–187 ISBN 978-3-540-17218-5.
181. Mauri, A.; Consonni, V.; Todeschini, R. Molecular Descriptors. In *Handbook of Computational Chemistry*; Leszczynski, J., Kaczmarek-Kedziera, A., Puzyn, T., G. Papadopoulos, M., Reis, H., K. Shukla, M., Eds.; Springer International Publishing: Cham, **2017**; 2065–2093 ISBN 978-3-319-27281-8.
182. Hoffman, K.; Kunze, R.A. *Linear Algebra*; 2d ed.; Prentice-Hall: Englewood Cliffs, N.J, **1971**; 407 ISBN 978-0-13-536797-1.
183. Diudea, M.V.; Cigher, S.; Vizitiu, A.E.; Florescu, M.S.; John, P.E. Omega Polynomial and Its Use in Nanostructure Description. *J. Math. Chem.* **2009**, *45*, 316–329, doi:10.1007/s10910-008-9408-1.
184. Polynomials calculator. Available Online: <https://www.symbolab.com/solver/polynomial-equation-calculator> (Accessed on 10 February 2024).
185. Matrix calculators. Available Online: <https://www.123calculus.com/en/matrix-permanent-page-1-35-160.html> (Accessed on 10 February 2024).
186. Matrix calculators. Available Online: <https://matrixcalc.org/> (Accessed on 10 February 2024).
187. Matrix calculators. Available Online: <https://matrix.reshish.com/determinant.php> (Accessed on 10 February 2024).
188. Rouvray, D.H. Graph Theory in Chemistry. *R. Inst. Chem., Rev.* **1971**, *4*, 173, doi:10.1039/rr9710400173.
189. Rouvray, D.H. The Search for Useful Topological Indices in Chemistry: Topological Indices Promise to Have Far-Reaching Applications in Fields as Diverse as Bonding Theory, Cancer Research, and Drug Design. *Am. Sci.* **1973**, *61*, 729–735.
190. Rask, A.E.; Huntington, L.; Kim, S.; Walker, D.; Wildman, A.; Wang, R.; Hazel, N.; Judi, A.; Pegg, J.T.; Jha, P.K.; et al. Massively Parallel Quantum Chemistry: PFAS on over 1 Million Cloud vCPUs. *arXiv* **2023**, doi:10.48550/ARXIV.2307.10675.
191. Houston, P.L.; Qu, C.; Yu, Q.; Conte, R.; Nandi, A.; Li, J.K.; Bowman, J.M. PESPIP: Software to Fit Complex Molecular and Many-Body Potential Energy Surfaces with Permutationally Invariant Polynomials. *J. Chem. Phys.* **2023**, *158*, 044109, doi:10.1063/5.0134442.
192. Li, Z.; Omidvar, N.; Chin, W.S.; Robb, E.; Morris, A.; Achenie, L.; Xin, H. Machine-Learning Energy Gaps of Porphyrins with Molecular Graph Representations. *J. Phys. Chem. A* **2018**, *122*, 4571–4578, doi:10.1021/acs.jpca.8b02842.
193. Dou, B.; Zhu, Z.; Merkurjev, E.; Ke, L.; Chen, L.; Jiang, J.; Zhu, Y.; Liu, J.; Zhang, B.; Wei, G.-W. Machine Learning Methods for Small Data Challenges in Molecular Science. *Chem. Rev.* **2023**, *123*, 8736–8780, doi:10.1021/acs.chemrev.3c00189.
194. Wang, T.Y.; Neville, S.; Schuurman, M. Machine Learning Seams of Conical Intersection: A Characteristic Polynomial Approach. *J. Phys. Chem. Lett.* **2023**, *14*, 7780–7786, doi:10.1021/acs.jpcllett.3c01649.
195. El-Basil, S. Caterpillar (Gutman) Trees in Chemical Graph Theory. In *Advances in the Theory of Benzenoid Hydrocarbons*; Gutman, I., Cyvin, S.J., Eds.; Topics in Current Chemistry; Springer Berlin Heidelberg: Berlin, Heidelberg, **1990**; Vol. 153, 273–289 ISBN 978-3-540-51505-0.
196. Knop, J.V.; Trinajstić, N. Chemical Graph Theory. II. On the Graph Theoretical Polynomials of Conjugated Structures. *Int. J. Quantum Chem.* **2009**, *18*, 503–520, doi:10.1002/qua.560180853.
197. Joița, D.-M.; Jäntschi, L. Extending the Characteristic Polynomial for Characterization of C₂₀ Fullerene Congeners. *Mathematics* **2017**, *5*, 84, doi:10.3390/math5040084.
198. Trinajstić, N. *Chemical Graph Theory*; 2nd ed.; CRC Press: Boca Raton Florida USA, **1992**; 322 ISBN 978-0-8493-4256-1.

199. Liu, S.; Zhang, H. On the Characterizing Properties of the Permanent Polynomials of Graphs. *Linear Algebra Appl.* **2013**, *438*, 157–172, doi:10.1016/j.laa.2012.08.026.
200. Ghosh, P.; Mandal, B. Formulas for the Characteristic Polynomial Coefficients of the Pendant Graphs of Linear Chains, Cycles and Stars. *Mol. Phys.* **2014**, *112*, 1021–1029, doi:10.1080/00268976.2013.828108.
201. Ghosh, P.; Klein, D.J.; Mandal, B. Analytical Eigenspectra of Alternant Edge-Weighted Graphs of Linear Chains and Cycles: Some Applications. *Mol. Phys.* **2014**, *112*, 2093–2106, doi:10.1080/00268976.2014.886737.
202. Mondal, S.; Mandal, B. Procedures for Obtaining Characteristic Polynomials of the Kinetic Graphs of Reversible Reaction Networks. *BCSJ* **2018**, *91*, 700–709, doi:10.1246/bcsj.20170381.
203. Mondal, S.; Mandal, B. Sum of Characteristic Polynomial Coefficients of Cycloparaphenylene Graphs as Topological Index. *Mol. Phys.* **2020**, *118*, e1685693, doi:10.1080/00268976.2019.1685693.
204. Gutman, I.; Vidović, D.; Furtula, B. Coulson Function and Hosoya Index. *Chem. Phys. Lett.* **2002**, *355*, 378–382, doi:10.1016/S0009-2614(02)00291-9.
205. Cash, G.G. Coulson Function and Hosoya Index: Extension of the Relationship to Polycyclic Graphs and to New Types of Matching Polynomials. *J. Math. Chem.* **2005**, *37*, 117–125, doi:10.1007/s10910-004-1444-x.
206. Cash Immanants and Immanantal Polynomials of Chemical Graphs. *J. Chem. Inf. Comput. Sci.* **2003**, *43*, 1942–1946, doi:10.1021/ci0300238.
207. Deford, D. *An Application of the Permanent-Determinant Method: Computing the Z-Index of Trees*; Technical Report Series; Washington State University: Pullman, **2013**.
208. Cash, G.G. The Permanent Polynomial. *J. Chem. Inf. Comput. Sci.* **2000**, *40*, 1203–1206, doi:10.1021/ci000031d.
209. Li, W.; Qin, Z.; Zhang, H. Extremal Hexagonal Chains with Respect to the Coefficients Sum of the Permanent Polynomial. *Appl. Math. Comput.* **2016**, *291*, 30–38, doi:10.1016/j.amc.2016.06.025.
210. Li, S.; Wei, W. Extremal Octagonal Chains with Respect to the Coefficients Sum of the Permanent Polynomial. *Appl. Math. Comput.* **2018**, *328*, 45–57, doi:10.1016/j.amc.2018.01.033.
211. Wei, W.; Li, S. Extremal Phenylene Chains with Respect to the Coefficients Sum of the Permanent Polynomial, the Spectral Radius, the Hosoya Index and the Merrifield–Simmons Index. *Discrete Appl. Math.* **2019**, *271*, 205–217, doi:10.1016/j.dam.2019.07.024.
212. Wu, T.; Lai, H.-J. On the Permanent Sum of Graphs. *Appl. Math. Comput.* **2018**, *331*, 334–340, doi:10.1016/j.amc.2018.03.026.
213. Huo, Y.; Liang, H.; Bai, F. An Efficient Algorithm for Computing Permanent Polynomials of Graphs. *Comput. Phys. Commun.* **2006**, *175*, 196–203, doi:10.1016/j.cpc.2006.03.002.
214. Botti, P.; Merris, R. Almost All Trees Share a Complete Set of Immanantal Polynomials. *J. Graph. Theory.* **1993**, *17*, 467–476, doi:10.1002/jgt.3190170404.
215. Randić, M.; Barysz, M.; Nowakowski, J.; Nikolić, S.; Trinajstić, N. Isospectral Graphs Revisited. *J. Mol. Struct.: THEOCHEM* **1989**, *185*, 95–121, doi:10.1016/0166-1280(89)85008-0.
216. Jiang, Y.; Liang, C. On Endospectral Bipartite Graphs. *Croat. Chem. Acta* **1995**, *68*, 343–357.
217. Hinze, J., Ed. *The Unitary Group for the Evaluation of Electronic Energy Matrix Elements*; Lecture Notes in Chemistry; Springer Berlin Heidelberg: Berlin, Heidelberg, **1981**; Vol. 22; 380 ISBN 978-3-540-10287-8.
218. Heidar-Zadeh, F.; Ayers, P.W.; Verstraelen, T.; Vinogradov, I.; Vöhringer-Martinez, E.; Bultinck, P. Information-Theoretic Approaches to Atoms-in-Molecules: Hirshfeld Family of Partitioning Schemes. *J. Phys. Chem. A* **2018**, *122*, 4219–4245, doi:10.1021/acs.jpca.7b08966.
219. Tomescu, M.A.; Jäntschi, L.; Rotaru, D.I. Figures of Graph Partitioning by Counting, Sequence and Layer Matrices. *Mathematics* **2021**, *9*, 1419, doi:10.3390/math9121419.

220. Chen, X.; Liu, M.; Gao, J. CARNOT: A Fragment-Based Direct Molecular Dynamics and Virtual-Reality Simulation Package for Reactive Systems. *J. Chem. Theory Comput.* **2022**, *18*, 1297–1313, doi:10.1021/acs.jctc.1c01032.
221. Lagrange, J.-L. Sur l'équation Séculaire de La Lune. *Mémoire de l'Académie royale des sciences de Paris* **1773**, 335–399.
222. Hückel, E. Quantentheoretische Beiträge zum Benzolproblem: I. Die Elektronenkonfiguration des Benzols und verwandter Verbindungen. *Z. Physik* **1931**, *70*, 204–286, doi:10.1007/BF01339530.
223. Hartree, D.R. The Wave Mechanics of an Atom with a Non-Coulomb Central Field. Part I. Theory and Methods. *Math. Proc. Camb. Phil. Soc.* **1928**, *24*, 89–110, doi:10.1017/S0305004100011919.
224. Hartree, D.R. The Wave Mechanics of an Atom with a Non-Coulomb Central Field. Part II. Some Results and Discussion. *Math. Proc. Camb. Phil. Soc.* **1928**, *24*, 111–132, doi:10.1017/S0305004100011920.
225. Fock, V. Näherungsmethode zur Lösung des quantenmechanischen Mehrkörperproblems. *Z. Physik* **1930**, *61*, 126–148, doi:10.1007/BF01340294.
226. Fock, V. „Selfconsistent field“ mit Austausch für Natrium. *Z. Physik* **1930**, *62*, 795–805, doi:10.1007/BF01330439.
227. Laplace, P.S. Additions Aux Recherches Sur Le Calcul Intégral et Sur Le Système Du Monde. *Mémoires de l'Académie royale des sciences de Paris* **1772**, 267–376,533–554.
228. Cauchy, A. Sur l'équation à l'aide de Laquelle on Détermine Les Inégalités Séculaires Des Mouvements Des Planets. *Exerc. Math.* **1829**, *4*, 140–160.
229. Slater, J.C. The Theory of Complex Spectra. *Phys. Rev.* **1929**, *34*, 1293–1322, doi:10.1103/PhysRev.34.1293.
230. Self-Consistent Field, with Exchange, for Beryllium. *Proc. R. Soc. Lond. A* **1935**, *150*, 9–33, doi:10.1098/rspa.1935.0085.
231. Sylvester, J. On the Theorem Connected with Newton's Rule for the Discovery of Imaginary Roots of Equations. *Messenger Math.* **1880**, *9*, 71–84.
232. Godsil, C.D.; Gutman, I. On the Theory of the Matching Polynomial. *J. Graph. Theory.* **1981**, *5*, 137–144, doi:10.1002/jgt.3190050203.
233. Godsil, C.D. Algebraic Matching Theory. *Electron. J. Combin.* **1995**, *2*, R8, doi:10.37236/1202.
234. Ramaraj, R.; Balasubramanian, K. Computer Generation of Matching Polynomials of Chemical Graphs and Lattices. *J. Comput. Chem.* **1985**, *6*, 122–141, doi:10.1002/jcc.540060207.
235. Curticapean, R. Counting Matchings of Size k Is $\sharp W[1]$ -Hard. In *Automata, Languages, and Programming*; Fomin, F.V., Freivalds, R., Kwiatkowska, M., Peleg, D., Eds.; Lecture Notes in Computer Science; Springer Berlin Heidelberg: Berlin, Heidelberg, **2013**; Vol. 7965, 352–363 ISBN 978-3-642-39205-4.
236. Schöning, U. Graph Isomorphism Is in the Low Hierarchy. *J. Comput. Syst. Sci.* **1988**, *37*, 312–323, doi:10.1016/0022-0000(88)90010-4.
237. King, R.B. Applications of Graph Theory and Topology for the Study of Aromaticity in Inorganic Compounds. *J. Chem. Inf. Comput. Sci.* **1992**, *32*, 42–47, doi:10.1021/ci00005a007.
238. Santos, J.C.; Andres, J.; Aizman, A.; Fuentealba, P. An Aromaticity Scale Based on the Topological Analysis of the Electron Localization Function Including σ and π Contributions. *J. Chem. Theory Comput.* **2005**, *1*, 83–86, doi:10.1021/ct0499276.
239. Herndon, W.C. Structure-Resonance Theory for Pericyclic Transition States. *J. Chem. Educ.* **1981**, *58*, 371, doi:10.1021/ed058p371.
240. Bruderer, M.; Contreras-Pulido, L.D.; Thaller, M.; Sironi, L.; Obreschkow, D.; Plenio, M.B. Inverse Counting Statistics for Stochastic and Open Quantum Systems: The Characteristic Polynomial Approach. *New J. Phys.* **2014**, *16*, 033030, doi:10.1088/1367-2630/16/3/033030.

241. Arguin, L.-P.; Belius, D.; Bourgade, P. Maximum of the Characteristic Polynomial of Random Unitary Matrices. *Commun. Math. Phys.* **2017**, *349*, 703–751, doi:10.1007/s00220-016-2740-6.
242. Lita Da Silva, J. On the Characteristic Polynomial, Eigenvectors and Determinant of Heptadiagonal Matrices. *Linear Multilinear Algebra* **2017**, *65*, 1852–1866, doi:10.1080/03081087.2016.1258034.
243. Von Collatz, L.; Sinogowitz, U. Spektren endlicher grafen: Wilhelm Blaschke zum 70. Geburtstag gewidmet. *Abh. Math. Semin. Univ. Hambg.* **1957**, *21*, 63–77, doi:10.1007/BF02941924.
244. Sloane, N.; Plouffe, S. Number of Graphs on n Unlabeled Nodes. *A000088, Formerly M1253 N* **1996**, 479.
245. Weisstein, E.W. Number of Unique Characteristic Polynomials among All Simple Undirected Graphs on n Nodes. *A082104* **2003**.
246. The IUPAC International Chemical Identifier: *CI -- Newsmagazine for IUPAC* **2006**, *28*, doi:10.1515/ci.2006.28.6.12.
247. Jäntschi, L.; Bolboacă, S.-D.; Furdui, C.M. Characteristic and Counting Polynomials: Modelling Nonane Isomers Properties. *Mol. Simul.* **2009**, *35*, 220–227, doi:10.1080/08927020802398892.
248. Jäntschi, L. Characteristic and Counting Polynomials of Nonane Isomers; Academic Direct Publishing House: Cluj-Napoca, Romania, **2007**; 100 ISBN 978-973-86211-3-8.
249. Putz, M.V., Mirica, M.C., Sustainable Nanosystems Development, Properties, and Applications. *Advances in Chemical and Materials Engineering; IGI Global*, **2017**; 793 ISBN 978-1-5225-0492-4.
250. Bolboacă, S.-D.; Jäntschi, L. Counting Distance and Szeged (on Distance) Polynomials in Dodecahedron Nano-Assemblies. In *Distance, Symmetry, and Topology in Carbon Nanomaterials*; Ashrafi, A.R., Diudea, M.V., Eds.; Springer International Publishing: Cham, **2016**; Vol. 9, 391–408 ISBN 978-3-319-31582-9.
251. Jäntschi, L. Online Calculation of Graph Polynomials Such as Counting Polynomial and Characteristic Polynomial. **2006**. Available Online: <http://l.academicdirect.org/Fundamentals/Graphs/polynomials/> (Accessed on 10 February 2024).
252. Gabor, B.M.; Vreman, P.P. Free Pascal: Open Source Compiler for Pascal and Object Pascal. **1988** (and to Date). Available Online: <https://www.freepascal.org/> (Accessed on 10 February 2024).
253. Hehre, W.J.; Ditchfield, R.; Pople, J.A. Self-Consistent Molecular Orbital Methods. XII. Further Extensions of Gaussian-Type Basis Sets for Use in Molecular Orbital Studies of Organic Molecules. *J. Chem. Phys.* **1972**, *56*, 2257–2261, doi:10.1063/1.1677527.
254. Jäntschi, L.; Bolboacă, S.-D. Performances of Shannon's Entropy Statistic in Assessment of Distribution of Data. *OUAC* **2017**, *28*, 30–42, doi:10.1515/auoc-2017-0006.
255. Jäntschi, L. Tests. Available Online: <http://l.academicdirect.ro/Statistics/tests/> (Accessed on 10 February 2024).
256. Fisher, R.A. Questions and Answers #14. *Am. Stat.* **1948**, *2*, 30–31.
257. Jäntschi, L.; Bolboacă, S.-D. Distribution Fitting 3. Analysis under Normality Assumption. *Bull. Univ. Agric. Sci. Vet. Med. Cluj-Napoca Hort.* **2009**, *66*, 698–705.
258. Student The Probable Error of a Mean. *Biometrika* **1908**, *6*, 1, doi:10.2307/2331554.
259. Welch, B.L. The Generalization of "Student's" Problem When Several Different Population Variances Are Involved. *Biometrika* **1947**, *34*, 28–35, doi:10.1093/biomet/34.1-2.28.
260. Sharma, E.; Panday, S.; Mittal, S.K.; Joița, D.-M.; Pruteanu, L.L.; Jäntschi, L. Derivative-Free Families of With- and Without-Memory Iterative Methods for Solving Nonlinear Equations and Their Engineering Applications. *Mathematics* **2023**, *11*, 4512, doi:10.3390/math11214512.
261. Joița, D.-M.; Tomescu, M.A.; Bălint, D.; Jäntschi, L. An Application of the Eigenproblem for Biochemical Similarity. *Symmetry* **2021**, *13*, 1849, doi:10.3390/sym13101849.

262. Huang, S.; Cole, J.M. A Database of Battery Materials Auto-Generated Using ChemDataExtractor. *Sci. Data* **2020**, *7*, 260, doi:10.1038/s41597-020-00602-2.
263. Battery Data. Available online: <https://www.materialsforbatteries.org/data/> (Accessed on 10 February 2024).
264. Dong, R.; Pan, S.; Peng, Z.; Zhang, Y.; Yang, J. mTM-Align: A Server for Fast Protein Structure Database Search and Multiple Protein Structure Alignment. *Nucleic Acids Res.* **2018**, 380–386, doi:10.1093/nar/gky430.
265. Kolodny, R.; Koehl, P.; Levitt, M. Comprehensive Evaluation of Protein Structure Alignment Methods: Scoring by Geometric Measures. *J. Mol. Biology* **2005**, *346*, 1173–1188, doi:10.1016/j.jmb.2004.12.032.
266. Terashi, G.; Takeda-Shitaka, M. CAB-Align: A Flexible Protein Structure Alignment Method Based on the Residue-Residue Contact Area. *PLoS ONE* **2015**, *10*, e0141440, doi:10.1371/journal.pone.0141440.
267. Akdel, M.; Durairaj, J.; de Ridder, D.; van Dijk, A.D.J. Caretta – A Multiple Protein Structure Alignment and Feature Extraction Suite. *CSBJ* **2020**, *18*, 981–992, doi:10.1016/j.csbj.2020.03.011.
268. Holm, L. Using Dali for Protein Structure Comparison. In *Structural Bioinformatics*; Gáspári, Z., Ed.; Methods in Molecular Biology; Springer US: New York, NY, **2020**; Vol. 2112, 29–42 ISBN978-1-07-160269-0.
269. Hu, J.; Liu, Z.; Yu, D.-J.; Zhang, Y. LS-Align: An Atom-Level, Flexible Ligand Structural Alignment Algorithm for High-Throughput Virtual Screening. *Bioinformatics* **2018**, *34*, 2209–2218, doi:10.1093/bioinformatics/bty081.
270. Menke, M.; Berger, B.; Cowen, L. Matt: Local Flexibility Aids Protein Multiple Structure Alignment. *PLoS Comput. Biol.* **2008**, *4*, 88–99, doi:10.1371/journal.pcbi.0040010.
271. Zhang, Y. TM-Align: A Protein Structure Alignment Algorithm Based on the TM-Score. *Nucleic Acids Res.* **2005**, *33*, 2302–2309, doi:10.1093/nar/gki524.
272. Chen, W.; Yao, C.; Guo, Y.; Wang, Y.; Xue, Z. pmTM-Align: Scalable Pairwise and Multiple Structure Alignment with Apache Spark and OpenMP. *BMC Bioinformatics* **2020**, *21*, 426, doi:10.1186/s12859-020-03757-2.
273. Shegay, M.V.; Suplatov, D.A.; Popova, N.N.; Švedas, V.K.; Voevodin, V.V. parMATT: Parallel Multiple Alignment of Protein 3D-Structures with Translations and Twists for Distributed-Memory Systems. *Bioinformatics* **2019**, *35*, 4456–4458, doi:10.1093/bioinformatics/btz224.
274. Dong, R.; Peng, Z.; Zhang, Y.; Yang, J. mTM-Align: An Algorithm for Fast and Accurate Multiple Protein Structure Alignment. *Bioinformatics* **2018**, *34*, 1719–1725, doi:10.1093/bioinformatics/btx828.
275. Holm, L. DALI and the Persistence of Protein Shape. *Protein Sci.* **2020**, *29*, 128–140, doi:10.1002/pro.3749.
276. Jäntschi, L. The Eigenproblem Translated for Alignment of Molecules. *Symmetry* **2019**, *11*, 1027, doi:10.3390/sym11081027.
277. Huang, J.; Zhang, M.; Ma, J.; Liu, X.; Kobbelt, L.; Bao, H. Spectral Quadrangulation with Orientation and Alignment Control. In Proceedings of the ACM SIGGRAPH Asia 2008 papers; ACM: Singapore, December **2008**; 1–9.
278. Abdelmoumen N. An Algebraic Solution to the Multilateration Problem. **2015**, *ReserchGate*, doi:10.13140/RG.2.1.1681.3602.
279. Zhao, C.; Sacan, A. UniAlign: Protein Structure Alignment Meets Evolution. *Bioinformatics* **2015**, *31*, 3139–3146, doi:10.1093/bioinformatics/btv354.
280. Xu, Z.; Huang, X.; Jimenez, F.; Deng, Y. A New Record of Graph Enumeration Enabled by Parallel Processing. *Mathematics* **2019**, *7*, 1214, doi:10.3390/math7121214.
281. Medina, L.; Nina, H.; Trigo, M. On Distance Signless Laplacian Spectral Radius and Distance Signless Laplacian Energy. *Mathematics* **2020**, *8*, 792, doi:10.3390/math8050792.

282. Hayat, S.; Khan, S.; Khan, A.; Liu, J.-B. Valency-Based Molecular Descriptors for Measuring the π - Electronic Energy of Lower Polycyclic Aromatic Hydrocarbons. *Polycycl. Aromat. Compd.* **2022**, *42*, 1113–1129, doi:10.1080/10406638.2020.1768414.
283. Hayat, S.; Khan, S. Quality Testing of Spectrum-Based Valency Descriptors for Polycyclic Aromatic Hydrocarbons with Applications. *J. Mol. Struct.* **2021**, *1228*, 129789, doi:10.1016/j.molstruc.2020.129789.
284. Abd-Rabo, M.A.; Zakarya, M.; Cesarano, C.; Aly, S. Bifurcation Analysis of Time-Delay Model of Consumer with the Advertising Effect. *Symmetry* **2021**, *13*, 417, doi:10.3390/sym13030417.
285. Jukic, S.; Saracevic, M.; Subasi, A.; Kevric, J. Comparison of Ensemble Machine Learning Methods for Automated Classification of Focal and Non-Focal Epileptic EEG Signals. *Mathematics* **2020**, *8*, 1481, doi:10.3390/math8091481.
286. Zhang, C.; Pei, D. Generalized Bertrand Curves in Minkowski 3-Space. *Mathematics* **2020**, *8*, 2199, doi:10.3390/math8122199.
287. Tirkolaei, E.B.; Dashtian, Z.; Weber, G.-W.; Tomaskova, H.; Soltani, M.; Mousavi, N.S. An Integrated Decision-Making Approach for Green Supplier Selection in an Agri-Food Supply Chain: Threshold of Robustness Worthiness. *Mathematics* **2021**, *9*, 1304, doi:10.3390/math9111304.
288. Wei, Y.; Zheng, Y.; Jiang, Z.; Shon, S. A Study of Determinants and Inverses for Periodic Tridiagonal Toeplitz Matrices with Perturbed Corners Involving Mersenne Numbers. *Mathematics* **2019**, *7*, 893, doi:10.3390/math7100893.
289. Pei, J.-T.; Bai, Y.-S. Lie Symmetries, Conservation Laws and Exact Solutions for Jaulent-Miodek Equations. *Symmetry* **2019**, *11*, 1319, doi:10.3390/sym11101319.
290. Gasiński, L.; Papageorgiou, N.S. Resonant Anisotropic (p,q)-Equations. *Mathematics* **2020**, *8*, 1332, doi:10.3390/math8081332.
291. Moaaz, O.; Furuichi, S.; Muhib, A. New Comparison Theorems for the Nth Order Neutral Differential Equations with Delay Inequalities. *Mathematics* **2020**, *8*, 454, doi:10.3390/math8030454.
292. Kamran, K.; Shah, Z.; Kumam, P.; Alreshidi, N.A. A Meshless Method Based on the Laplace Transform for the 2D Multi-Term Time Fractional Partial Integro-Differential Equation. *Mathematics* **2020**, *8*, 1972, doi:10.3390/math8111972.
293. Sharma, J.R.; Kumar, S.; Jäntschi, L. On a Class of Optimal Fourth Order Multiple Root Solvers without Using Derivatives. *Symmetry* **2019**, *11*, 1452, doi:10.3390/sym11121452.
294. Kumar, D.; Sharma, J.R.; Jäntschi, L. A Novel Family of Efficient Weighted-Newton Multiple Root Iterations. *Symmetry* **2020**, *12*, 1494, doi:10.3390/sym12091494.
295. Materials Data on Ca₂Si by Materials Project 2020.
491. Shakerzadeh, E.; Azizinia, L. Can C₂₄N₂₄ Cavernous Nitride Fullerene Be a Potential Anode Material for Li-, Na-, K-, Mg-, Ca-Ion Batteries? *Chem. Phys. Lett.* **2021**, *764*, 138241, doi:10.1016/j.cplett.2020.138241.
492. Nematollahi, P.; Neyts, E.C. Linking Bi-Metal Distribution Patterns in Porous Carbon Nitride Fullerene to Its Catalytic Activity toward Gas Adsorption. *Nanomaterials* **2021**, *11*, 1794, doi:10.3390/nano11071794.
493. Hahn, Th., Ed.; Space-Group Symmetry in *International Tables for Crystallography*; 1st ed.; International Union of Crystallography: Chester, England, **2006**; Vol. A; 938 ISBN 978-0-7923-6590-7.
494. The MathWorks Inc.; *MATLAB 2020 9.8.0.1323502 (R2020a)*. Natick, Massachusetts, United States.